

SPECIAL ISSUE: STATE OF BAY-DELTA SCIENCE 2022

Remote Sensing of Primary Producers in the Bay-Delta

Erin Hestir^{*1}, Iryna Dronova²

ABSTRACT

Remote-sensing methods are being used to study a growing number of issues in the San Francisco Estuary, such as (1) detecting the optical properties of chlorophyll-*a* concentrations and dissolved organic matter to assess productivity and the nature of carbon inputs, (2) creating historical records of invasive aquatic vegetation expansion through space and time, (3) identifying origins and expansions of invasions, and (4) supporting models of greenhouse-gas sequestration by expanding restoration projects. Technological capabilities of remote sensing have likewise expanded to include a wide array of opportunities: from boat-mounted sensors, human-operated low-flying planes, and aerial drones, to freely accessible satellite imagery. Growing interest in coordinating these monitoring methods in the name of collaboration and cost-efficiency has led to the creation of diverse expert teams such as the Remote Imagery

Collaborative, and monitoring frameworks such as the Interagency Ecological Program Aquatic Vegetation Monitoring Framework and Wetland Regional Monitoring Program. This paper explores the emerging technologies and applications of various methods for studying primary producers, with an emphasis on remote sensing.

KEY WORDS

remote sensing, satellite, UAS, multispectral, hyperspectral, LiDAR, SAR, primary producers, vegetation, phytoplankton

INTRODUCTION

Over the past 4 decades, the availability and use of satellite observations of the Earth's land surface and its oceans have transformed our understanding of primary production and the global carbon cycle (Xiao et al. 2019; Brewin et al. 2021). Sensors mounted on satellite platforms have provided synoptic, systematically repeated measurements over the Earth's oceans and continents. The data have enabled (1) assessments of the spatial patterns and temporal variability of primary producers, (2) estimates of primary productivity, and (3) improvements of primary productivity models. Recent advances in sensor instruments, platform technologies,

SFEWS Volume 20 | Issue 4 | Article 5

<https://doi.org/10.15447/sfews.2023v20iss4art5>

* Corresponding author: ehestir@ucmerced.edu

1 University of California, Merced
Merced, CA 95343 USA

2 University of California, Berkeley
Berkeley, CA 94720 USA

and computing tools—coupled with a concerted intergovernmental effort to advocate free and open data—have increased the availability of remotely-sensed data products at finer spatial, temporal, and spectral scales (GEO 2015). Thus, our ability to observe complex ecosystems such as those of the San Francisco Estuary (encompassing the San Francisco Bay, Suisun Marsh, and Sacramento–San Joaquin Delta; hereafter “estuary”) has also increased. Remote sensing is now widely recognized as a key measurement technique to assess and monitor primary producers and primary productivity.

In the estuary, remote sensing is a powerful and cost-effective tool to enrich ongoing research efforts on primary producers in a geospatially explicit context, often with regular, repeated sampling that enables measurements of seasonal and longer-term variability. Because remote sensors often make tens to hundreds of distinct measurements across the electromagnetic spectrum, the data have high information content that is spatially explicit and can be used to simultaneously estimate and map multiple parameters of interest, such as chlorophyll-*a*, colored dissolved organic matter, suspended sediments, and the discrimination of phytoplankton functional types in the water column (Palacios et al. 2015; Fichot et al. 2016; Jensen et al. 2019). Remote sensing allows for synoptic sampling across relatively large areas (depending on the platform), thus enabling systematic and simultaneous measurements across both terrestrial and aquatic domains and ecosystems at the land–water interface, such as wetlands, which are notoriously difficult to access via boat, foot, or other vehicle (Wu 2018). No other measurement technology affords such cross-domain advantages and the ability to collect data over inaccessible areas. Finally, remote sensing provides a powerful complement to *in situ* observations, which provide detailed but highly localized information, and may be sparsely distributed in space or time or both (Balsamo et al. 2018).

What is Remote Sensing? A Beginner's Guide

There are as many definitions of remote sensing as there are texts on the subject, encompassing the broad (obtaining information at a distance) to the narrow (imaging conducted by satellites or aircrafts), with many different variations in between.

In this paper, we define remote sensing as the measurement of reflected and emitted electromagnetic radiation from the surface of the Earth via a sensor mounted on a remote platform (such as a satellite). Such measurements are then converted to more meaningful biogeophysical variables (such as radiance or reflectance, elevation, or even chlorophyll concentration) through the application of algorithms.

Remote sensing can be classified into two broad categories: **passive** and **active**.

- **Passive**, or optical remote sensing, such as satellite and aerial photography, measures the naturally available energy. Measurements are made in two dominant wavelength regions: (1) the ultraviolet, visible, near-infrared, and shortwave-infrared region where the sun is reflected from the Earth's surface, and (2) the longwave thermal to microwave region emitted from Earth.
- **Active sensors**, such as LiDAR, radar and sonar, provide their own energy source and then measure the intensity and time of the return, enabling inference about surface roughness, elevation, bathymetry and more.

Most of the sensors operating around the world today are passive sensors (Khorram et al. 2012). Through analysis of spectral reflectance and emissivity, we can make inferences about the composition and temperature of materials on the Earth's surface for every pixel in an image. For primary producers, this includes plant and phytoplankton functional types (including harmful algal blooms and invasive species), species or genus identification and distribution, chlorophyll-*a* and other accessory pigments, photosynthetic pathways, biomass, foliar chemistry and stress, biodiversity, habitat types and associated environmental conditions (Hestir et al. 2015).

The Ecosystem of Sensing

To conduct remote-sensing measurements, sensors are mounted on platforms such as satellites, airplanes, or unoccupied aircraft. Sensors, including cameras and spectrometers, may also be mounted on fixed platforms, which are often co-located with micrometeorological eddy-covariance flux instrumentation. *In situ* observations and *in situ* sensing are a critical part of the sensing ecosystem (Figure 1). Human-

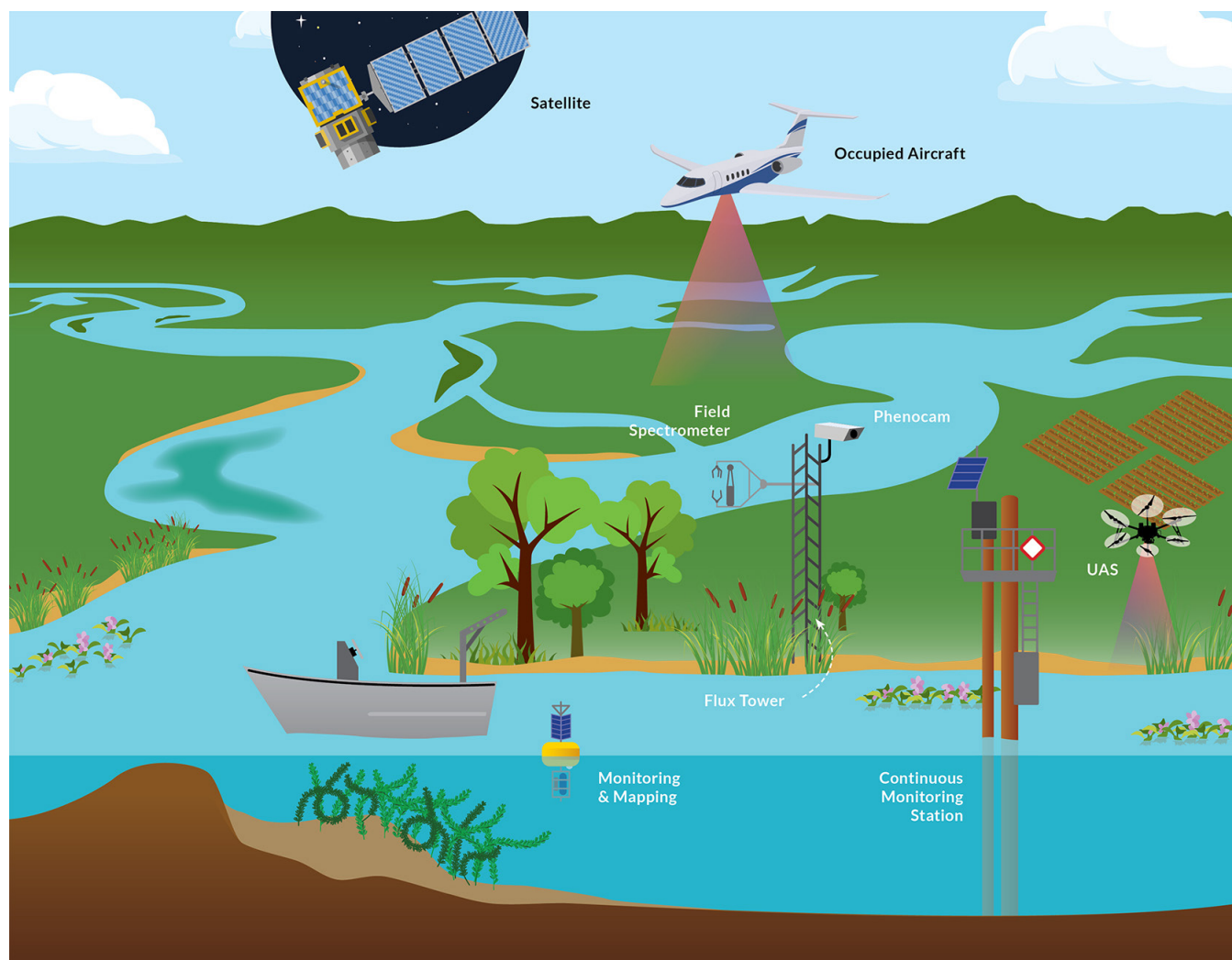


Figure 1 The ecosystem of sensing the San Francisco Estuary. *Illustrated by Vincent Pascual with the California Office of State Publishing.*

led *in situ* observations are often an integral component of the remote-sensing analysis chain, often serving as calibration or training data when mapping primary producers and estimating primary productivity. *In situ* observations are often used to quantify uncertainty for remotely-sensed products, a necessary step that provides the basis for using measures to assess prescribed objectives for many management applications (Ciriello et al. 2021). These observations may also provide important complementary information that is unobtainable from remote sensing directly, such as the data collected by eddy-covariance flux towers or species composition of plant communities. In the estuary and Delta waters, *in situ* water-quality sensing via sensor networks—

such as the continuous monitoring stations maintained by the California Department of Water Resources (CDWR) and the US Geological Survey (USGS)—have been critical to the calibration and validation of remotely-sensed water-quality products, and provide additional information on the physical and chemical conditions of the water column (Ade et al. 2021; Gustine et al. 2021; Halverson et al. 2021; Lee et al. 2021). PhenoCams are time-lapse photography instrumentation that provide high-temporal-frequency local image observations. A growing number of eddy-covariance greenhouse-gas flux towers coupled with PhenoCams provide distributed information about micrometeorology, carbon exchange, and vegetation dynamics (Knox et al. 2015; Knox et

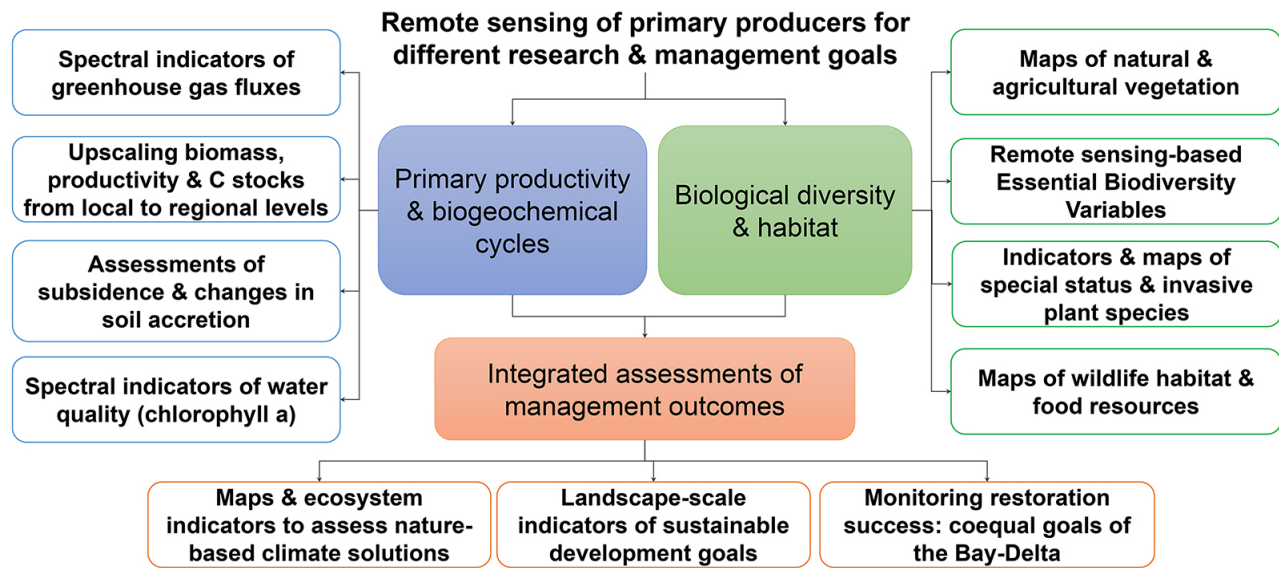


Figure 2 Remote sensing of primary producers in relation to different research and management goals in the estuary

al. 2017; Dronova et al. 2021). High-throughput *in situ* sensing via high-speed watercraft can rapidly map large areas for a key suite of aquatic physical and biogeochemical parameters (Downing et al. 2017; Kraus et al. 2017), providing an excellent complement to regional remote-sensing products (Fichot et al. 2016).

The Need and Management Context for Remote Sensing of Primary Producers

There is a converging need for primary producer assessments across multiple state, national, and international initiatives (Figure 2), such as the Ramsar Convention on Wetlands, the United Nations (UN) Convention on Biological Diversity (CBD), and California's Executive Order N-82-20 established by Gavin Newsom's administration in 2020 to initiate the California Biodiversity Collaborative. Both the US Environmental Protection Agency (USEPA) and California Water Code drive a need for water-column algal monitoring. The Delta's co-equal goals of preserving a reliable water supply and ecosystem restoration while maintaining unique cultural values, including agriculture (DSC 2019), and the state's goals for reducing greenhouse gas (GHG) emissions (SB 2) (Deverel et al. 2017), closely echo the UN's Sustainable Development

Goals for clean water, climate action, protection, preserving life on land and below water, and supporting sustainable communities and economic growth.

Because of the multi-faceted role that primary producers play in estuarine ecological functions and ecosystem services, remote sensing helps meet the needs of many different management questions and objectives. Primary producers are a critical component of ecological food webs that are a central focus of research and management efforts to conserve biodiversity, protect and restore ecological habitats, and predict the responses to environmental change of ecological populations and trophic chains (Figure 2). Remote sensing can be used to monitor the status of ecological communities and habitats shaped by primary producers from the aquatic to upland domains, and to project their responses to climate change and inform adaptive management efforts. Landscape-scale assessments, as well as monitoring and management efforts, require vegetation and habitat mapping at high levels of both spatial and ecological detail (e.g., plant species and communities), which is becoming increasingly feasible with advances in high-spatial and high-spectral remote sensing, image-

processing methods, and machine learning. Management priorities that focus on trophic relationships and threats to their ecological integrity often require primary producer biomass and productivity to be modeled, which can be facilitated by remote sensing-based maps and spectral indicators of photosynthetically active biomass. In aquatic settings, this extends to remotely-sensed indicators of algal productivity, which has additional relevance to water-quality management. Whereas, higher spectral resolution, which provides the capability to measure narrow spectral features critical to differentiating plant functional types and water column pigments, comes with a trade-off of reduced spatial resolution or reduced radiometric resolution. The latter is critical for water-column remote sensing (Price 1997; Hestir et al. 2015; Dierssen et al. 2021).

Categories of Remote Sensing of Primary Producers

Remote sensing of primary producers to meet management needs falls into several categories that differ in terms of data resolution and the intensity and scope of data processing. These categories include (1) mapping, (2) measuring, and (3) modeling. **Mapping** goals refer to representation of certain thematic categories in the landscape, including vegetation (i.e., categorical data). Datasets to support mapping goals need to be spatially explicit and should be able to highlight not only the presence of vegetation components, but also more nuanced distributions of target species, communities, and habitats, while conforming to mapping accuracy standards. Repeated mapping over time that maintains similar accuracy and error levels is critical for robust monitoring and assessment of changes in primary producer distribution and characteristics (Hickson and Keeler-Wolf 2007; Hestir et al. 2012; Taddeo et al. 2019).

Measuring applications extract information from a pixel's spectral data, sometimes coupled with information about the spatial arrangement of pixels. These spectral data are then used to either directly estimate a specific parameter, such as chlorophyll-*a* concentration, or indirectly estimate parameters such as biomass or leaf area index (LAI) through proxies such as the popular

normalized difference vegetation index (NDVI) (Byrd et al. 2014; Dronova and Taddeo 2016; Knox et al. 2017). Finally, remote sensing can be used to support ecosystem **modeling**, wherein remotely-sensed proxies for primary producers are integrated with other data sets and models that characterize ecosystem function (Anderson et al. 2016; Baldocchi et al. 2016; Oikawa et al. 2017; Anderson et al. 2018; Eichelmann et al. 2018). Given the diverse objectives of such analyses, the choice of remote-sensing system and approach often needs to be tailored to a given management application, as discussed in more detail below.

Resolution Considerations

The utility of remote sensing for studying primary producers is largely a function of the data set's resolution relative to the study or management application's objective. Different phenomena and processes associated with primary productivity—from photosynthesis to ecological invasions and plant succession—occur at different scales across time and space and are best measured by different types of remote-sensing modalities. In turn, remote-sensing resolution is governed by the properties of the sensor as well as the platform on which it is mounted. Remote-sensing resolution is typically characterized by four different types of resolution: (1) **spatial resolution**, defined as the ground area captured by a single pixel, is a measure of the image clarity; (2) **spectral resolution** is the number, width, and sometimes range of the intervals over which the electromagnetic spectrum is measured; (3) **temporal resolution** is the frequency of a measurement; and (4) **radiometric resolution** is the lowest level of radiance or reflectance a sensor can measure at each spectral band.

In general, design trade-offs between different facets of remote-sensing resolution must be considered when selecting the appropriate data set for a given application. Kennedy et al. (2009) provide a detailed overview of concepts and trade-offs specific to landscape monitoring. As a rule of thumb, the spatial resolution and areal footprint of an image are determined by the altitude of the platform on which the sensor is mounted, as well as the properties of the sensor itself. As the

altitude of the platform increases, so does the capability to image a larger area of the Earth's surface, but the spatial resolution decreases. This trade-off means that sensors mounted on unoccupied aerial vehicles (UAVs) and occupied (i.e., piloted) aircraft provide much higher spatial resolution (i.e., smaller pixels), but cover a much smaller footprint than a sensor mounted on a satellite. Higher *spatial* resolution often comes at a cost of lower *spectral* resolution because the amount of energy received by the detector is finite.

The trade-offs between platforms also affect the temporal resolution of a remote-sensing observation. Satellites are often desired platforms because, when in low Earth polar orbit, they provide regular repeat observations every 2 to 16 days. The frequency of the revisit is a function of the altitude of the platform and the swath width of the sensor, which again also affects spatial resolution and footprint size; increased temporal frequency results in increased swath size, and thus increased spatial *footprint*, but decreased spatial *resolution*. Occupied aircrafts and UAVs provide the advantages of higher spatial resolution and user-defined data acquisition timing. However, the cost of deploying such technologies at scale across the Delta remain extremely high (Bolch et al. 2021).

Most medium- to coarse-spatial-resolution satellite data sets (10 m to 1 km) are also often desirable to researchers because the data are often provided at no cost to the user by open-access providers such as the National Aeronautic and Space Administration (NASA), the National Oceanic and Atmospheric Administration (NOAA), the USGS, and the European Space Agency (ESA). Higher-spatial-resolution satellite data sets are most often commercial and may have to be tasked to acquire a specific scene of interest, often at a cost. However, the Commercial Remote Sensing Space Policy has enabled US federal and civil agencies to work together to identify user needs and leverage commercial satellite assets. As a result, the Commercial Data Purchases Imagery Collection hosted by the USGS enables qualified federal users to obtain commercial satellite data

at no cost (<https://www.usgs.gov/centers/eros/science/usgs-eros-archive-commercial-satellites-commercial-data-purchases-cdp-imagery>), though licensing restrictions often apply.

Spatial Resolution

Very-coarse-spatial-resolution data sets (e.g., MODIS [Moderate Resolution Imaging Spectroradiometer], 1-x-1-km pixel size) have been used to map and model terrestrial and marine primary productivity at the global scale for decades (Ryu et al. 2011; Tao et al. 2017; Groom et al. 2019; Brewin et al. 2021). However, such spatial resolution is widely viewed as one of the primary factors that limit applying remote sensing to estuarine, coastal, and inland aquatic and wetland ecosystems, as well as to detecting invasive species (Ozesmi and Bauer 2002; Hestir et al. 2008; Turpie et al. 2015; Bolch et al. 2020). The coarser pixels generally appropriate for marine and large-scale forestry applications do not capture narrow river channels, fine water features, spatially complex ecosystems, small patches of primary producers, and nascent invasive plant species patches—all characteristic of the Delta, Suisun Marsh, and other marsh-like complexes of the estuary. While coarse-resolution data can provide information on general spatial patterns and gradients, it can obscure inference about productivity hotspots and vegetation density, and may lead to difficult-to-quantify errors in remote-sensing products such as spectral vegetation indices (SVIs) used to derive estimates of net primary productivity (NPP). **Figure 3** illustrates the effects of spatial resolution on a commonly used spectral index, the NDVI, at a wetland site in the western Delta. The NDVI was calculated from imagery obtained from the California National Agriculture Imagery Program (NAIP) collected in 2018 at 0.6-m spatial resolution. The data were then resampled to 1-m, 10-m, 30-m, 100-m, 250-m, and 500-m pixel size to the wetland site boundary (shown in red), overlaid on the grayscale background of the original NAIP image. Resampling and clipping were performed in ArcGIS (Esri) Desktop version 10.8 using, respectively, Aggregate and Extract by Mask tools, which preserved only NDVI pixels with their center inside the site boundary.

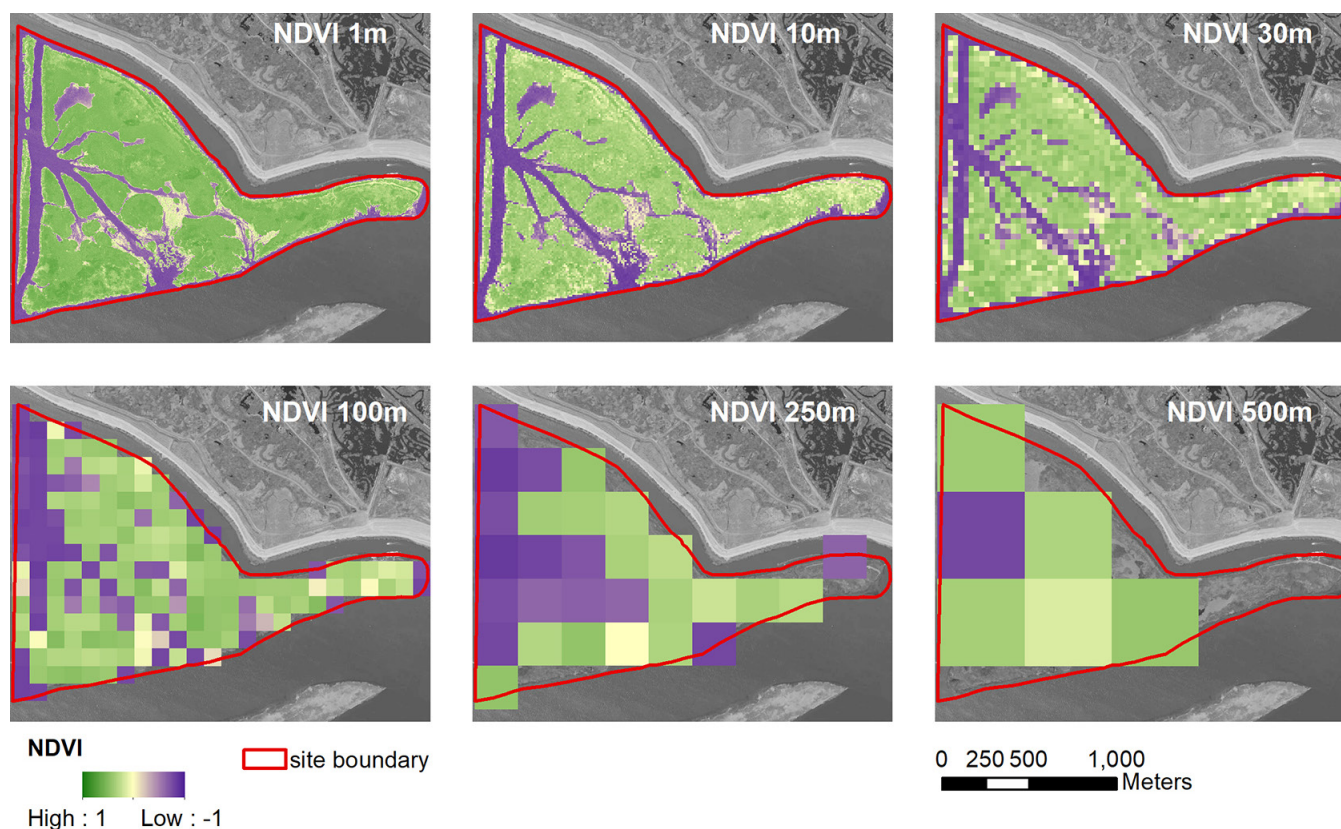


Figure 3 The effects of spatial resolution on mapping the Normalized Difference Vegetation Index (NDVI). The different panels show the effects of resampling high-resolution data to larger sizes at a wetland site in the western Delta.

Hestir et al. (2008) and Ta et al. (2017) recommend pixel sizes less than 5 x 5 m to map floating and submerged aquatic vegetation (FAV and SAV) in the Delta. Most management needs that focus on FAV mapping seek genus-level and species-level maps, which necessitates such high spatial resolution (Khanna et al. 2012; Santos et al. 2016; Khanna et al. 2018). Such high-resolution data can only be acquired from aircraft or commercial high-spatial-resolution satellites. In cases where species- and genus-level mapping are not needed, pixel sizes of 30 m or less are sufficient for many wetland and salt marsh mapping applications (Turpie et al. 2015; Byrd et al. 2018; Muller-Karger et al. 2018). In the Delta, recent work has shown that 30-x-30-m pixels from Landsat and 20-x-20-m pixels from Sentinel-2 can be used to map wetlands, FAV and SAV, and rice paddies (Baldocchi et al. 2016; Ta et al. 2017; Ade et al. 2022), and to track changes in spectral indicators of primary production (Anderson et al. 2016).

The uncertainty in delineating primary producer distributions tends to increase with coarser grain or larger pixel size (Kelly et al. 2011). The effect of larger pixel sizes leads to the mixed pixel problem, wherein multiple different-vegetation types or landcover types are present in a single pixel, all represented by one spectral measurement. The mixed-pixel problem affects all three applications of remote sensing of primary producers: mapping, measuring, and modeling. Mixed pixels lead to classification errors when primary producers are mapped—sparse and rare vegetation classes decrease in abundance or disappear, abundant classes become more dominant, and the mean patch size tends to increase when pixel size increases (Saura 2002; Bolch et al. 2021). This effect is illustrated in Figure 4, in which a vegetation map produced from piloted-aircraft imaging spectroscopy (i.e., “hyperspectral” remote sensing) at 1.7-m pixel resolution is compared with a map produced from

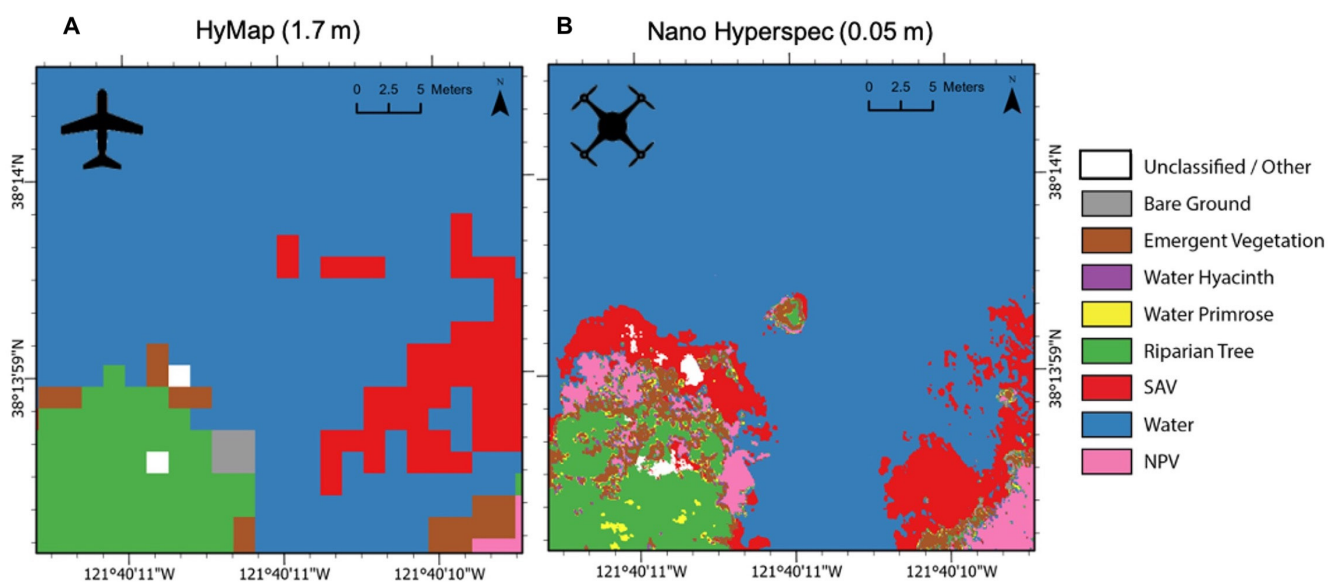


Figure 4 The effects of pixel size on class occurrence and abundance. (A) HyMap hyperspectral sensor mounted on a manned aircraft (1.7-m pixel resolution). (B) Nano Hyperspec hyperspectral sensor mounted on an unmanned aerial vehicle (UAV) (0.05-m pixel resolution). Source: Figure modified from Bolch et al. (2021).

an imaging spectrometer mounted on a UAV with data collected at 0.05-m resolution. Furthermore, while coarser resolution generally leads to poorer mapping accuracy, the effect is not always linear, and often depends on the heterogeneity of the landscape as well as the design and geolocational precision and accuracy of field data (Knight and Lunetta 2003; Frazier 2015).

The mixed-pixel problem affects remote-sensing measurements of both aquatic and terrestrial chlorophyll-*a* and other proxies such as NDVI. As pixel size increases, the spatial information content of the data decreases logarithmically (Tarnavsky et al. 2008) and no longer conforms to the boundaries of landscape units of interest, such as wetland land parcels, as illustrated in Figure 3. Further, mixed pixels can lead to both large random errors (as much as 100%), as well as bias errors (i.e., estimation offsets) in remote-sensing-derived and remote-sensing-modeled estimates of LAI, NPP, and algal blooms (Simic et al. 2004; Xu et al. 2004; Lekki et al. 2019). Larger pixels also inhibit water-column chlorophyll-*a* measurements because narrow channels cannot be resolved: there is no way to tell how much

chlorophyll-*a* comes from the land, and how much from the water.

The question then remains: *What is the appropriate spatial resolution for remote sensing of primary producers?* In principle, the minimum mapping unit (MMU) should define the appropriate spatial resolution. The MMU is the size of the smallest feature that is present on a map. If the feature is smaller than the MMU, it will not be shown on the map. The MMU will vary based on the application or management need. For example, the MMU for mapping primary productivity in rice fields in California will be larger than the MMU for mapping primary productivity in Delta marshes, given that the average size of a farm in California is ~140 ha (CDFA 2020), whereas the average patch size of marsh is ~4 ha (Robinson et al. 2014). If individual tree-crown mapping is the objective, the MMU will be either the anticipated average or lower quantile dimensions of the tree crowns in the study. The VegCAMP (2015) report provides more detailed guidance for MMU definition, but still leaves the final decision to the discretion of the project. Once MMU is defined, the spatial resolution of remote-sensing imagery

should be less than the MMU, although exact recommendations are not easily found in the literature. One study suggested spatial resolution should be spatial resolution $\leq \sqrt{MMU/\kappa}$, where κ is a conversion coefficient ranging from 0.53 to -0.85 (L Li et al. 2019). However, this recommendation is not widely cited or used.

In practice, the availability and cost of data often dictates spatial resolution, as well as other trade-offs related to temporal and spectral resolution. For instance, medium-resolution satellite data (e.g., Landsat 30 m) are often selected both for their data accessibility (often free and open access) and data availability (based on temporal resolution). With such data there are solutions to the mixed-pixel problem for both primary producer detection and NPP mapping or modeling. Soft—or fuzzy—classification methods that assign each pixel different degrees of membership in several classes are often used to address the mixed-pixel problem. The most notable of these techniques is spectral mixture analysis, which models each pixel spectra as a linear combination of pure spectra of its landscape components (“endmembers;” e.g., bare soil, water, or vegetation), and thus enables each pixel to be mapped as fractions of different endmembers (Franke et al. 2009; Frazier

and Wang 2011). This technique has been used successfully in the salt marsh and freshwater marshes in the San Francisco Bay and Delta (H Li et al. 2005; Rosso et al. 2005; Byrd et al. 2014) and is an integral component in the aquatic-invasive-species mapping framework used by UC Davis (Hestir et al. 2008; Khanna et al. 2018). The number of endmembers that can be successfully modeled is constrained by the number of spectral bands in remote-sensing data; the higher the spectral resolution, the more detailed and accurate the spectral mixture analysis will be.

Finally, biomass- and productivity-focused modeling efforts are also sensitive to the spatial scale of remote-sensing inputs (Byrd et al. 2018; Dronova et al. 2021). This issue may be addressed by using different-resolution remote-sensing products simultaneously; for instance, Byrd et al. (2018) reported an improvement of tidal vegetation biomass modeling from 30-m Landsat satellite imagery after including the fraction of green vegetation derived from 1-m aerial products from the US Department of Agriculture’s (USDA) NAIP. In another study that modeled evapotranspiration over the whole Delta, Anderson et al. (2018) combined 30-m Landsat imagery with lower-temporal-resolution (8 to 16 days) and daily coarser-resolution MODIS

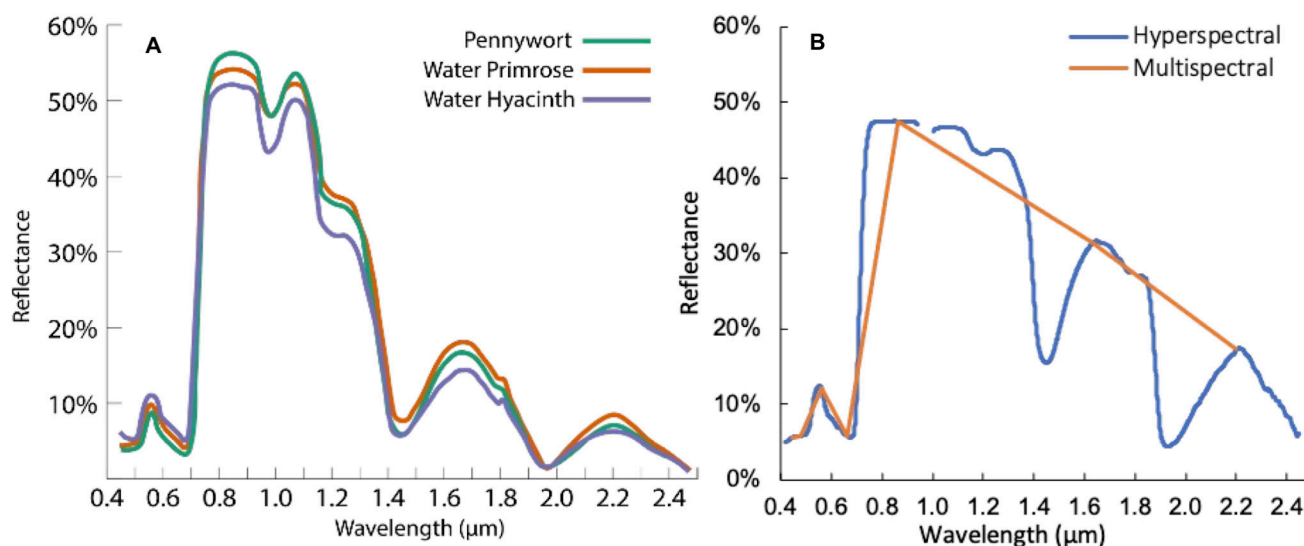


Figure 5 (A) The reflectance spectrum of three floating aquatic vegetation (FAV) species in the Delta. The fine spectral detail from high-resolution hyperspectral remote sensing enables discrimination of different FAV to the genus and species level. (B) The hyperspectral and multispectral reflectance of a green leaf. Sources: Data from S. Khanna and the USGS.

products to characterize the seasonality of plant function and canopy leaf area.

Spectral Resolution

All primary producers have some traits in common; most notably from a remote-sensing perspective they possess photosynthetic pigments. Chlorophyll and other accessory pigments, the structure of the cells and/or leaves, and the structure of the water column or canopy all dominate different regions of the spectral signal (Figure 5). Species with similar functions typically have similar pigment composition and structure, and thus tend to have more similar spectral signals. High-spectral-resolution data—sometimes called hyperspectral—provides the ability to better discriminate primary producer communities and functional types, and even discriminate between different genera and species in both terrestrial and aquatic systems of the estuary (Rosso et al. 2005; Hestir et al. 2012; Khanna et al. 2012; Santos et al. 2012; Khanna et al. 2018). High-spectral-resolution data also enable estimates of biochemical composition and other important traits related to photosynthetic processes, water content, leaf area index, and canopy structure (Ustin and Gamon 2010; Santos et al. 2012; Homolová et al. 2013). In the water column, high-spectral-resolution data are critical to differentiating chlorophyll-*a* from other water-quality constituents, which enable mapping of phytoplankton functional types and potentially harmful algal blooms (Ryan et al. 2014; Dierssen et al. 2015; Kudela et al. 2015; Dierssen et al. 2021).

Imaging spectroscopy makes measurements in very narrow intervals nearly contiguously across the optical spectrum, enabling detailed high-resolution spectra at every pixel. Multispectral remote sensing makes just a few measurements across a broader portion of the electromagnetic spectrum. While less spectral information is contained in multispectral data, these data sets form the bulk of currently available, free, open-access remote-sensing data sets, although this is changing (see “Looking Ahead: The Very Near Future of Remote Sensing of Primary Producers in the Estuary”). Multispectral data provide valuable information about landcover (Clark 2017), the extent and distribution of wetlands (Quinn and Epshtein 2014), different vegetation communities and plant functional types (Villa et al. 2015; Ade et al. 2022), and even wetland biodiversity (Taddeo et al. 2019). Multispectral information can also be used to assess the physiological status of plants, primarily using spectral indexes, such as the NDVI. Such indexes, when coupled with a time-series of measurements, provide important information about the phenology and dynamics of vegetation communities (Taddeo and Dronova 2019; Dronova et al. 2021) and are used to infer or model biomass and primary productivity (Byrd et al. 2014; Byrd et al. 2018), as described in other papers in this special issue.

The number of spectral bands, their width, and their position vary across sensors (Figure 6), which can greatly influence the comparability of spectral indexes across data sets—uncertainty

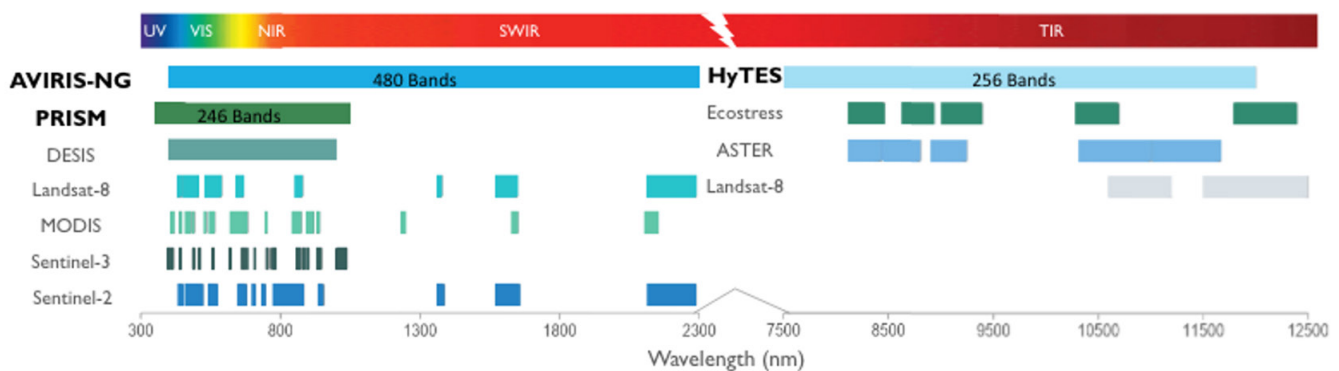


Figure 6 A comparison of spectral band widths and positions. Hyperspectral sensors, such as AVIRIS, PRISM and HyTES, provide many narrow measurements for contiguous coverage across a range of the electromagnetic spectrum. *Source: Jacob Nesslage, UC Merced.*

that is difficult to quantify because there is no direct validation available for a spectral index (Huang et al. 2021). This uncertainty is further compounded by differences in spatial resolution across sensors, which means the footprint is not the same between images taken over the same geographic region. For example, a recent study showed that the NDVI calculated from five different airborne and satellite sensors over the same study area varied from 0.4 to 0.9 (on a scale of -1 to 1) (Huang et al. 2021). In the Sacramento–San Joaquin Delta, Dronova et al. (2021) compared phenology metrics (start of greening, end of greening, etc.) derived from a spectral index from two sensors: Landsat and a high-spatial-resolution commercial satellite. They found that phenological metrics varied by 10 to 79 days, and the agreement between different satellite inputs was non-systematic.

Fortunately, harmonization between different sensor data sets is advancing, leading to seamless image products that provide a unified data set with a denser time-series (Claverie et al. 2018). Once such harmonized products are widely available, it may be possible to have consistent measurements across multiple satellite sensors that have different spectral resolution. This will also result in higher-temporal-resolution data sets through the formation of “virtual constellations.” For example, combining Landsat 8 and Sentinel-2 data results in a ~2.9-day revisit frequency. Harmonizing the data between Landsat 8 and Sentinel-2 has been shown to be successful for monitoring terrestrial phenology (Bolton et al. 2020) and measuring water-column total suspended solids (Pahlevan et al. 2019). However, the uncertainties from harmonized products have yet to be sufficiently quantified for remote sensing of primary producers in the estuary.

Temporal Resolution

As with spatial resolution, temporal resolution should be defined by the needs of the application but is often limited by the reality of what free and open-access data are available. Mapping vegetation to track the distribution of changes in emergent aquatic vegetation (EAV), FAV, and SAV communities and various wetland habitats in the

estuary may only necessitate an annual time-step or greater, thus requiring the relatively low temporal resolution (but high spatial resolution) afforded by commercially contracted aircraft and high-spatial-resolution commercial satellites (e.g., Chapple and Dronova 2017; Khanna et al. 2018). However, the timing of data acquisition is critical. The best time of year to map species and biomass is generally recognized to be during the growing season, and optimally when key species of interest are showing the greatest phenological differences, such as when flowering (Andrew and Ustin 2006; Adam et al. 2010; Wan et al. 2019).

If the application requires quantification in the change of primary producers over time, particularly to understand changes in production, then multiple observations are necessary before, during, and after an event. For example, quantifying the phenological events of green-up and senescence of primary producers typically requires temporal resolution on the order of 6 to 16 days or higher, and the probability of error in derived metrics increases by up to 20% with greater temporal gaps between sequential observations, e.g., because of clouds (Zhang et al. 2009). Tracking changes in water-column primary producers requires an even higher temporal resolution. For example, remote sensing of phytoplankton requires a temporal resolution on the order of hours to days to capture dynamic changes, particularly in tidal systems such as the estuary (Mouw et al. 2015; Muller-Karger et al. 2018).

High temporal resolution also increases the likelihood of collecting data at the “right time” for a given application, particularly from satellite platforms. For example, wetlands and aquatic vegetation are hydrodynamically variable, and water influences the spectral signal very strongly. Variations in water level can shift the red-edge absorption or red-edge reflectance features of vegetation (Turpie 2013). Thus, water level influences many of the diagnostic spectral indexes used to estimate biomass, NPP, or vegetation phenological status and health (although, this may be overcome with water-adjusted indexes, e.g., Villa et al. 2014). Variations

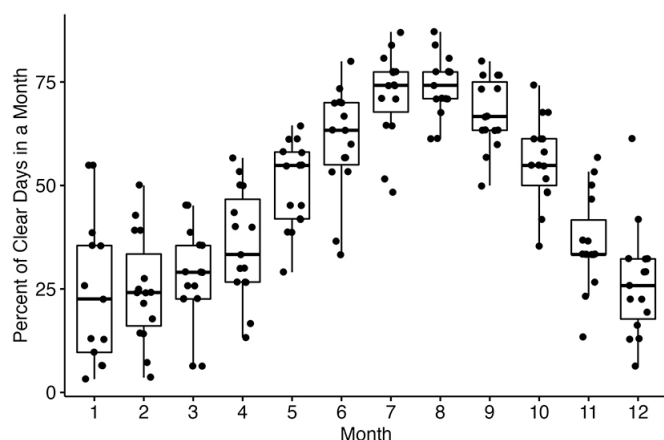


Figure 7 The number of low or no-cloud cover days (<10% fractional cover) by month from 2003 to 2017 for the San Francisco Bay and Sacramento-San Joaquin Delta, calculated via the NASA Aqua satellite's Atmospheric Infrared Sounder (AIRS) Monthly Standard Physical Retrieval cloud cover product

in water level and water quality can also influence the capability to detect SAV, and thus acquiring data at low tide is recommended (Hestir et al. 2008). High-temporal-resolution data also increases the likelihood of collecting cloud-free data, a critical consideration when dealing with optical remote sensing.

Hestir et al. (2015) provide two definitions of temporal resolution for optical remote sensing data. The first is the **designed resolution** determined by the platform altitude and orbit (e.g., 16 days for Landsat), and the second is the **effective resolution**, which is determined by the region's cloudiness. At the global scale, a satellite repeat frequency with a designed resolution of 16 days (e.g., Landsat) provides at least seasonal effective temporal resolution. Given the climate conditions of California, there are many cloud-free days throughout the year, increasing the effective temporal resolution for all satellite remote-sensing missions in the estuary relative to other regions. However, there is a seasonal bias in the cloud-free conditions over the region. We estimate there are an average of 168.5 days (± 15.6 days) each year with low or no cloud cover for the estuary. As expected, this statistic varies a great deal monthly and interannually,

particularly during winter (Figure 7). These estimates were obtained using the NASA Aqua satellite's Atmospheric Infrared Sounder (AIRS) Monthly Standard Physical Retrieval cloud cover product. We further calculated that the probability of any 1 day in the year having low (<10%) or no cloud cover is 58%. This means the likelihood of at least monthly cloud-free data from a 16-day repeat interval for the estuary is higher than the global average (Mercury et al. 2012), but with strong seasonality that may lead to a seasonal bias in data density. However, higher temporal frequency can increase the likelihood of a cloud-free scene. Thus, the Sentinel-2 satellites, with a combined temporal resolution of 5 days and the virtual constellation of Sentinel-2 plus Landsat (with a combined temporal resolution of 2.9 days), provide an appealing opportunity for remote sensing of primary producers in the estuary. Another solution is active sensing technology, such as light detection and ranging (LiDAR) and synthetic aperture radar (SAR), which do not depend on reflected sunlight for the measurement, and can thus be used under cloudy conditions, or even at night.

Radiometric Resolution and Sensor Fidelity

Radiometric resolution—the signal-to-noise ratio of the sensor—and the radiometric dynamic range are critical resolution requirements for remote sensing of water-column primary producers. This is because water very effectively absorbs electromagnetic radiation: very little signal returns to the sensor. Thus, the sensitivity of the sensor can affect the accuracy of water-column chlorophyll-*a* estimates, a key component of the primary production in aquatic systems. This can be accounted for by spatial or spectral binning (Giardino et al. 2007; Vanhellemont and Ruddick 2014), which presents another trade-off consideration for aquatic applications. Higher-spatial-resolution sensors capable of imaging the waterways of the estuary (e.g., Landsat, Sentinel-2, Airborne Visible/Infrared Imaging Spectrometer Classic [AVIRIS-c]) are designed for terrestrial applications. This means they do not have the radiometric resolution or sensitivity to discriminate between low concentrations of chlorophyll-*a* typically found

in the estuary and optically confounding water-column constituents such as suspended solids and dissolved organic matter. However, next-generation sensors—including Landsat 8, Landsat 9, and new hyperspectral airborne and satellite instruments—have the spatial, spectral, and radiometric resolution and sensitivity suited to accurately retrieve water-column primary producers (Giardino et al. 2019).

Other Remote Sensing Modalities

While most remote-sensing data used in the estuary is passive optical remote sensing, active instruments such as (LiDAR) and (SAR) have been useful for remote sensing of primary producers. LiDAR—most often mounted on aircraft, but also increasingly on UAV—can characterize the 3-dimensional (3-D) structure of the vegetation canopy as well as the topography of the underlying surface. Canopy structure and microtopography have been used to discriminate salt-marsh species and invasive wetland species (Rosso et al. 2006; Andrew and Ustin 2008), identify wetland ecotones and controls on invasive species phenology (Andrew and Ustin 2009a), and model potential species invasions (Andrew and Ustin 2009b). However, the density of salt-marsh vegetation limits the laser penetration of the canopy and thus introduces uncertainty in wetland digital elevation models (Rosso et al. 2006). In contrast with the discrete laser pulses of most commercially deployed LiDAR systems, full waveform LiDAR records the entire backscattered signal from the laser pulse, thus providing more information on salt-marsh vegetation structure and density (Rogers et al. 2015) and potentially more accurate estimates of surface elevation (Rogers et al. 2018). However, full-waveform LiDAR data acquisitions have not yet been conducted in the estuary to our knowledge.

SAR, mounted on both airborne and spaceborne platforms, measures backscattered microwave radiation sideways along a flightpath. Because of its ability to penetrate canopies, SAR has been used extensively around the world to detect and map forested wetlands (Henderson and Lewis 2008) and to monitor the extent of surface water and wetland inundation (Brisco 2015). In the

Delta, it has been used to improve the mapping of crops and rice paddies (Torbick et al. 2011; H Li et al. 2019) and to assess flood embankments (Wood et al. 2018), levee stability, and subsidence (Bekaert et al. 2019), but it has not yet been used extensively to map or model primary producers.

Measuring Change through Time

One of the most desirable aspects of remote sensing to study primary producers is the capability to make repeated, systematic measurements over time. This enables us to study ecological succession and invasion, primary producer responses to stressors or management treatments, and the effects of seasonality, weather, and climate on primary production. For example, the near-annual acquisition of airborne hyperspectral remote sensing has resulted in time-series maps of FAV and SAV. However, such a program is costly, and there is no dedicated monitoring program for aquatic vegetation in the Delta. Indeed, there was a 6-year gap in monitoring the Delta (2009 to 2013), and monitoring from 2016 to 2020 was curtailed to the northwest and central Delta because of limited funding. Yet the multi-user community recognizes the value in such a program, and there have been multiple calls for a consistent monitoring program using hyperspectral data (Boyer and Sutula 2015; Ta et al. 2017).

The most notable archival data set to study change through time is the Landsat series of satellite sensors, with Landsat 1 dating back to 1972. While Landsat data have been available to the scientific and management community since then, costs varied between \$200 and \$4,000 per scene, placing long-term time-series analysis out of reach for most (Wulder et al. 2012). The free and open-access Landsat data policy enacted in 2008 resulted in an explosion of users and applications, skyrocketing from ~1 million image downloads in 2009—the first year of the new policy—to 20 million in 2017 (Zhu et al. 2019). The Landsat data policy has since prompted similar policies around the world, such as free and open-access data from the ESA Copernicus program (i.e., Sentinel satellite data). It has also led to the development of third-party platforms

Table 1 Major satellite and selected aerial remote sensing systems applicable to the estuary. See Ustin and Middleton (2021) for a thorough discussion of the many satellite instruments of broad interest to ecological and environmental applications.

Type	Sensor or mission	Agency	Frequency	Temporal scope	Spatial resolution	Spectral sensitivity or related features
Passive (optical and thermal)	MODIS on Aqua and Terra satellites	NASA	Twice daily per sensor	2000–present	250–1000 m	Visible, near-infrared, and shortwave-infrared, thermal
	Landsat satellites	NASA	8–16 days	1972–present	30–120 m	
	ASTER (Terra satellite)	NASA	16 days	2000–present		
	Sentinel-2	ESA	5 days between 2 sensors	2015–present	10–30 m	Visible, near-infrared, and shortwave-infrared
	SPOT	ESA	~26 days	1986–present	1.5–20 m	
	NAIP (National Agriculture Imagery Program, aerial)	USDA	Every 2–3 years	Since 2005 in California	0.6–1 m	Visible and near-infrared
	PlanetScope satellites	PlanetLabs	~Daily	2015–present	3 m	Visible and near-infrared
	RapidEye	PlanetLabs	1–6 days	2008–present	5 m	Visible and near-infrared, red edge
	Commercial high resolution (e.g., IKONOS, Pleiades, WorldView, QuickBird)	Maxar	Variable; 3–140 days	Since ~2001	≤4 m	Often visible and near-infrared; additional visible and red-edge sensitivity in some (WorldView-2, WorldView-3, WorldView-4)
	PRISMA	Italian Space Agency (ASI)	7–14 days	2019–present	30 m	Hyperspectral
	DESI	German Space Agency (DLR)	3–5 days	2018–present	30 m	
	HISUI	Japan Space Agency	2–60 days	2019–present	20–30 m	
	AVIRIS (aerial)	NASA	Custom (tasked)	Since 2007 in the estuary	3–20 m in past data sets	
	HyMap	HyVista	Custom (tasked)	Since 2004 in the estuary	1.7–3 m	
	Hyperspectral Imager for the Coastal Ocean (HICO)	NASA	Custom (tasked)	2009–2014	90 m	
OCO-3	NASA	Daily	2019–present	≤4,000 m	Near-infrared and shortwave-infrared	
Ecostress	NASA	1–7 days	2018–present	70 m	Thermal infrared	
Active radar	ENVISAT ASAR	ESA	35 days	2002–2012	30–150 m for regional applications	Some of the SAR instruments collect data in different microwave spectra, view angles and polarizations, which increases the data information content
	RADARSAT satellites program (commercial)	Canadian Space Agency	4–24 days depending on mission	1995–present	10–100 m	
	Sentinel-1	ESA	6–12 days	2014–present	5–40 m depending on product	
	UAVSAR	NASA	Custom (tasked)	Since 2007	~6 m	
Active LiDAR	GEDI (satellite)	NASA	Variable, location-specific	2018–present	25–1,000 m depending on product and location	Full-waveform LiDAR
	Aerial LiDAR	Various	Custom	Different regions of the estuary since ~2003	Variable	Discrete-return (point cloud) LiDAR in most regional applications

such as Google Earth Engine and the Australian Commonwealth Scientific and Industrial Research Organisation (CSIRO) Open Data Cube Project, which provide petabytes of data and cloud-based computing platforms accessible through application programming interfaces to enable analyses across its entire archive. These platforms along with the long-term archival capabilities of Landsat now enable decadal-scale analyses of vegetation dynamics and management actions in the Delta (Taddeo and Dronova 2020).

REMOTE SENSING OF PRIMARY PRODUCERS TO MEET MANAGEMENT NEEDS

Mapping and Measuring Primary Producers

The mapping needs for primary producers in the estuary are primarily driven by management needs for baseline assessment and monitoring, tracking invasions, and monitoring and evaluating restoration. While some applications require very high spatial and spectral detail, such as mapping primary producers at a high level of taxonomic or functional detail (e.g., 5-m pixel resolution or less), plant cover or habitat distribution may be mapped at a variety of high to moderate spatial resolutions (10 to 30 m). While high-accuracy maps can often be made using a snapshot single-date observation, multi-temporal imagery is highly desirable for tracking change through time. Various studies in other regions have successfully exploited multi-temporal satellite remote sensing to achieve higher classification accuracy, particularly when phenological signals vary between classes (Bolch et al. 2020). It has been suggested that such an approach may be useful in the Delta (Hestir et al. 2008). However, this may have limited utility for mapping highly motile species such as FAV and may confound change detection because of variability between growing seasons (Tuxen et al. 2011).

Primary producers are usually mapped using classification techniques that may be manual, automated, or a combination of both. For example, California VegCAMP maps are often made through manual digitization and image segmentation of high-spatial-resolution NAIP aerial imagery, supported by reference information about

vegetation from rigorous field surveys (CDFW 2020). Other remote-sensing mapping techniques are more automated and use supervised classification techniques that require user input to define classes and training data for subsequent classification (Hestir et al. 2008; Khanna et al. 2011; Tuxen et al. 2011; Santos et al. 2016). When data have high spatial resolution but poor spectral resolution (e.g., aerial photography, UAV imagery, and some commercial high-spatial-resolution satellite data), object-based image analysis or texture metrics may be used to improve classification performance. Texture metrics in image analysis summarize tonal variability in an image from canopy heterogeneity and shadowing (Franklin et al. 2001). Object-based image analysis is a mapping workflow which first groups pixels into local regions (“objects”) and then classifies such regions to recover larger patches of vegetation and other surface types (Hossain and Chen 2019). Both texture metrics and object-based image analysis have been used to improve classification mapping of the estuary (Tuxen and Kelly 2008; Dronova et al. 2012; Moffett and Gorelick 2013; Chapple and Dronova 2017; Bolch et al. 2021). Finally, advanced machine learning techniques—such as classification and regression trees, random forests, support vector machines and neural networks—have shown considerable promise in recent years to improve recognition of landscape types from remote-sensing data. These techniques enable rapid and more automated approaches for high-accuracy mapping of aquatic vegetation functional types and species, and for modeling salt marsh vegetation aboveground biomass (Hestir et al. 2012; Byrd et al. 2018; Bolch et al. 2021).

Detecting and measuring primary producers often relies on the earlier mentioned spectral vegetation indices (SVIs) as biophysical indicators of primary producer pigments, structure, biomass or coverage, and canopy water content. SVIs are mathematical combinations of passive spectral reflectance signals from narrowband (hyperspectral) or broadband (multispectral) data. By design, SVIs prioritize portions of the electromagnetic spectrum that indicate plant function, such as the unique, vegetation-specific

utilization of solar radiation (Gitelson et al. 2006; Ustin and Gamon 2010; Ollinger 2011). For example, the popular NDVI capitalizes on the difference between the red region with strong photosynthetic absorption driven by leaf pigments and the near-infrared region with strong reflectance driven by plant cell structure (Rouse et al. 1974). Another popular SVI, the Enhanced Vegetation Index (EVI), incorporates reflectance in a shorter-wavelength blue region, which accounts for atmospheric aerosol effects (Huete et al. 2002). EVI is particularly beneficial in landscapes where signals from longer wavelengths saturate, such as closed-canopy forests and some aquatic and wetland environments (Knox et al. 2017; Taddeo et al. 2019). Temporal variability in SVIs provides important insights into the phenological dynamics of primary producers that shape the seasonality of different ecosystem functions (Matthes et al. 2015; Eichelmann et al. 2018; Dronova et al. 2021). Besides being useful as measurement proxies for the biophysical conditions of plants, SVIs are often used as inputs into multivariate classification schemes to map primary producers.

Data-fusion approaches that combine different remote-sensing data types also present an opportunity to improve mapping by providing more or additional information that spans different regions of the spectrum, incorporates active and passive techniques, or encompasses multiple resolutions. Hyperspectral remote sensing combined with LiDAR provides both the spectral information and structural information to accurately map *Salicornia* and invasive *Lepidium latifolium* (Rosso et al. 2006; Andrew and Ustin 2008). Multispectral data combined with LiDAR have also been used to improve digital elevation models (Buffington et al. 2016). However, given the vegetation zonation and organization of many tidal marshes, such data fusion is not always necessary (Moffett and Gorelick 2013).

The Water Column

Within the Water Column

Primary production by phytoplankton represents one of the most important sources of carbon flux

in the world, and forms the base of the aquatic food web. Satellite remote sensing of chlorophyll-*a* has long been used as a basis to model net primary production; recent advances in sensor spectral and radiometric resolution as well as algorithm advances have led to our ability to map and monitor phytoplankton functional groups and track potentially harmful algal blooms (Bracher et al. 2017). However, there are very few studies of remote sensing of water-column chlorophyll-*a* or phytoplankton functional groups in the estuary.

Detecting chlorophyll-*a* in coastal and inland waters is complicated by several factors. Only about 10% of the radiance measured at the top of the atmosphere is from the water signal; the remainder is from scattering in the atmosphere and reflections from the sun and sky. Thus, an important initial data-processing step is removing the effect of atmospheric gasses and particles from the water-leaving signal, a step more challenging in inland and coastal waters than for open ocean waters (Moses et al. 2017). Another major issue is the optical complexity of the water column, in which colored dissolved organic matter and total suspended solids confound traditional algorithm approaches for mapping chlorophyll-*a* and solar-induced fluorescence (Gilerson et al. 2007; Muller-Karger et al. 2018). Palacios et al. (2015) demonstrated that phytoplankton functional types can be mapped using airborne imaging spectroscopy in the nearby Monterey Bay, although atmospheric correction and sensor sensitivity were large sources of error in that study. Current satellite remote-sensing systems that have the spectral and radiometric resolution as well as the sensor fidelity necessary to detect phytoplankton pigment are not suited for coastal and inland waters because of limitations in spatial resolution. Mouw et al. (2015) provide a recent overview of these challenges for remote sensing of optically complex waters, and Diersssen et al. (2021) provide a complement to this review with a focus on hyperspectral remote sensing.

Another challenge for the estuary is the relatively low amount of chlorophyll-*a* in the water column, which affects retrieval accuracy. Hoogenboom

et al. (1998) used simulations with the AVIRIS hyperspectral instrument to show that the accuracy of chlorophyll-*a* retrieval greatly depends on the concentration of chlorophyll-*a* in the water column, and that this accuracy varies as a function of instrument sensitivity (from 10% error for concentrations greater than 12 mg m⁻³ to 33% error for concentrations of 2 mg m⁻³). Given the typically low concentrations of chlorophyll-*a* in much of the estuary, the capability to detect chlorophyll-*a* or other phytoplankton pigments at low concentrations is especially challenging. Fichot et al. (2016) overcame this limitation using the airborne Portable Remote Imaging Spectrometer (PRISM) imaging spectrometer, a hyperspectral system designed with high radiometric resolution for aquatic applications. Their chlorophyll-*a* retrievals were within ±13% to 18% of chlorophyll-*a* proxy measurement made with an *in situ* optical instrument, and within ±60% of actual chlorophyll-*a* concentrations. However, they also made the point that this does not prevent the detection of phytoplankton blooms when chlorophyll-*a* concentrations are increased several-fold, and ultimately concluded that remote sensing could be used to support water-quality monitoring and management in the estuary. Subsequently, satellite remote sensing has been used to support water-quality monitoring to inform management decisions about water operations and to assess short and long-term trends in fish habitat suitability (Ade et al. 2021; Gustine et al. 2021; Halverson et al. 2021; Lee et al. 2021), but only for turbidity and surface temperature.

Above and Below the Water Column

Remote sensing for invasive SAV and FAV has been significantly advanced by airborne hyperspectral campaigns flown nearly annually at low-tide conditions. In 2003, the Division of Boating and Waterways (DBW) funded the Center for Spatial Technologies and Remote Sensing (CSTARS) at UC Davis to implement a pilot project that mapped IAV in the Delta using airborne imaging spectroscopy (Underwood et al. 2003). After the success of the pilot project, the DBW provided funding for another 5 years, 2004 to 2008, to map plant communities across

the legal Delta every summer. This was started again in 2014 and has continued through 2021, using funds from NASA, the CDFW (California Department of Fish and Wildlife), the CDWR (California Department of Water Resources), and the DSC (Delta Stewardship Council). The data are acquired on low-altitude aircraft, enabling high-spatial-resolution (1.7- to 3-m pixel size) mapping of FAV to the genus/species level, and SAV to the functional-type level (Hestir et al. 2008; Khanna et al. 2011; Hestir et al. 2012; Khanna et al. 2012, 2018). Santos et al. (2012) demonstrated that it was possible to discriminate invasive from native growth forms of SAV using spectral data, and applied such techniques to image data, but this has not been extensively mapped for the Delta because of the heterogeneous mixtures of invasive and native species and a lack of species-level field data sufficient for extensive calibration and validation. Maps of FAV and SAV have underpinned critical invasion studies in the Delta, including the effectiveness of herbicide management and drought barriers (Santos et al. 2009; Khanna 2010; Kimmerer et al. 2019), ecological drivers and implications of biological invasions (Khanna et al. 2012; Santos et al. 2012; Santos et al. 2016; Khanna et al. 2018), and their effect on water quality and physical habitat (Hestir et al. 2016; Khanna et al. 2018).

Recent advances in platform and sensor technology are eliciting new possibilities for multi-scale mapping of FAV to the genus/species level in the Delta. The ESA's recent launch of the Sentinel-2 satellites provide multispectral data at 20-m spatial resolution every 5 days. Ade et al. (2022) recently demonstrated that machine learning can be used to discriminate water hyacinth and water primrose using Sentinel-2 data with comparable accuracy to airborne hyperspectral data, but with the loss of small patch detection. UAVs and miniaturized imaging spectrometers are leading to centimeter-scale mapping capabilities for targeted area applications. Bolch et al. (2021) used machine learning for UAV-mounted hyperspectral remote sensing to discriminate to the species/genus level of water hyacinth and water primrose with high accuracy. However, the utility of UAV to detect IAV

will not be in system-wide monitoring; because of the small footprint of UAV platforms, it would take over 7,000 hours of flight time to cover the entire area of the legal Delta (Bolch et al. 2021).

Wetlands and Marshes

Remote sensing has long been used to map the wetlands and marshes in the estuary (Zhang et al. 1997). These maps have been useful in assessing post-restoration recovery and vegetation colonization. Many applications of remote sensing for wetland restoration have highlighted the importance of regular remote-sensing monitoring. Such monitoring has enabled researchers to track the dynamics of premature senescence and variable colonization rates that may be obscured in regular field-based approaches (Tuxen et al. 2008). Remote sensing has also enabled researchers to quantify the effect of drought on vegetation development at a South Bay Salt Pond restoration site (Chapple and Dronova 2017). With the long-term archival capabilities of the Landsat sensor, spatial variability in wetland change can be quantified over time, which has led to an improved understanding of the importance of local context and fluctuations in the abiotic environment as factors in determining restoration outcomes (Taddeo and Dronova 2019).

In wetland and marsh ecosystems, most primary producers are also foundation species, meaning they provide critical habitat and serve as important drivers in the trophic web. Remote sensing of primary producers can thus also be used to assess the habitat potential and suitability of important species. Remotely sensed maps of marsh vegetation, canopy height, and geomorphology have been used to model avian habitat use and potential (Seavy et al. 2009; Stralberg et al. 2010). Such applications also extend to the water column. For example, LiDAR data have been used to quantify the effect of riparian tree shade on Delta surface waters, and to identify potential thermal refugia for spawning fish (Greenberg et al. 2012); and SAV maps from airborne hyperspectral remote sensing have been used to design a survey to investigate the association between SAV biomass and Largemouth Bass in the Delta (Conrad et al. 2016).

MODELING PRIMARY PRODUCTIVITY

Remote-sensing assessments of primary producers support regional ecological modeling efforts in two important ways: (1) using **maps**—the spatial extent and distribution of ecosystem components with thematic categories as different ecosystem functions (e.g., maps of vegetation types) and (2) using **measurements**—i.e., remote sensing-derived biophysical indicators of ecosystem properties and functions that primary producers control. Thematic maps that represent specific plant communities and crop types are often used to up-scale ecosystem functions such as primary productivity or greenhouse gas sequestration from discrete field data. The basic approach associates map categories with functional properties that are often assumed to be constant within such categories. For example, field-based chamber measurements of greenhouse gas emissions from wetlands can be used in concert with very-high-spatial-resolution (~15 cm) maps of vegetation and open water to greenhouse gas budgets across large, restored wetland sites (McNicol et al. 2017). Baldocchi et al. (2016) used multi-year maps of expanding rice paddies on Twitchell Island produced by 30-m Landsat satellite imagery to model changes in evapotranspiration. At a broader regional scale, Landsat and MODIS satellite products have been used to model evapotranspiration at scales relevant to the dynamics of Delta land uses (Anderson et al 2018).

Remote sensing-derived biophysical indicators can be used to model some ecosystem-level variables, such as biogeochemical fluxes and gross and net primary productivity (GPP and NPP, respectively). Biophysical indicators derived from SVIs are often used to empirically model ecosystem-level primary productivity and other ecosystem functions. Not surprisingly, SVIs have shown strong empirical correlations with wetland vegetation biomass (Byrd et al. 2014), canopy leaf area index (Dronova and Taddeo 2016), and indicators of GPP and net ecosystem exchange (NEE) for CO₂ (Matthes et al. 2015; Knox et al. 2017) among others. Additionally, the 3-D structure and biomass of vegetation can be directly measured with active remote-sensing

tools, such as LiDAR (Rosso et al. 2006) and high-resolution radar (H Li et al. 2019; Duncanson et al. 2020). However, the use of active remote sensing to directly measure biomass and model radiative transfer and primary productivity has been limited to date based on availability and the high costs of acquiring such data.

Remote Sensing-Based Modeling of Primary Producer Biomass and Ecological Functions

The Water Column

To date, regional applications of remote sensing for modeling primary producers have predominantly emphasized above-ground vegetation (mainly EAV) and ecosystem-wide assessments (Table 2). In contrast, primary productivity modeling of water column, mudflat, and below-water environments have been scarce, despite their advances in other estuaries and marine settings, including other California estuaries (Paterson et al. 1998; Zimmerman 2003; Méléder et al. 2020). Examples of relevant aquatic applications stop at mapping and may extend to studies of water quality (Catts et al. 1985; Fichot et al. 2016; Hestir et al. 2016).

Wetlands and Marshes

Modeling Primary Productivity and Biogeochemical Fluxes. Efforts to model primary producer biomass and productivity in emergent above-ground (above-water) and below-ground domains report strong empirical relationships between ecological variables and remote-sensing indicators from a wide array of sensors (Table 1). Notably, such applications involve both landscape-scale remote-sensing observations from satellite and airborne platforms and *in situ* sensing using spectroscopic instruments and PhenoCams. Matthes et al. (2015) used field spectroscopic measurements to compare seasonal dynamics between similarly structured, yet phenologically contrasting, canopies of a drained pasture and a rice paddy in the Delta. They also developed predictive models for GPP and NEE based on narrowband reflectance in visible and near-infrared regions and field ecosystem measurements. The seasonal dynamics of GPP and NEE have been also modeled in freshwater restored wetlands in the

Delta using vegetation greenness indices from Landsat imagery (Anderson et al. 2016) and with phenoCams (Knox et al. 2017). However, Anderson et al. (2016) also noted interannual discrepancies between NDVI and productivity, attributing them to potential confounding effects of variable green biomass coverage and background reflectance from water, soil, etc., which become inevitable because of pixel mixing at 30-m pixel resolution (Byrd et al. 2014; Dronova and Taddeo 2016). In such efforts, phenology of SVIs gains special importance both as an indicator of seasonality in primary producer function and as an indirect indicator of structural heterogeneity (Dronova et al. 2021).

Increasing spatial resolution of accessible remote-sensing data sets provides a breakthrough in up-scaling of primary productivity and biogeochemical budgets from point measurements by eddy-covariance stations (Baldocchi et al. 2001). These stations are equipped with specialized instruments that measure atmospheric concentrations of the target chemicals at high temporal frequencies along with relevant meteorological parameters such as atmospheric temperature, solar radiation, soil moisture, and others. Atmospheric concentrations of chemicals such as greenhouse gases represent a particular “footprint” of the contributing landscape area—the orientation and size of which can vary in time (Anderson et al. 2016; Knox et al. 2017)—that historically has required eddy-covariance stations to be placed within “homogenous” ecosystems. Spatial complexity and patchiness of estuarine landscapes creates uncertainty in interpreting and budgeting such field measurements, since temporal variation in measured fluxes becomes a function not only of the local photosynthesis and ecosystem respiration, but also of changes in the proportions of vegetation and other surfaces when the footprint shifts. Remote sensing-based maps of eddy-covariance footprints solve this problem, particularly when produced at sufficiently high spatial resolution. Matthes et al. (2014) demonstrated this by using different-season images of high-spatial-resolution commercial satellite data (WorldView-2), which was classified

into emergent vegetation, aquatic vegetation, and open water to parse annual variability in CH₄ fluxes based on changes in these landscape cover types.

Finally, increasing the temporal resolution of remote-sensing data will improve our ability to model primary productivity over time. Emerging remotely sensed phenological products, such as 30-m gridded measures of annual vegetation seasonality derived from harmonized Landsat and Sentinel-2 satellite data for North America (Bolton et al. 2020), are highly promising to streamline modeling primary productivity and other seasonally variable aspects of ecosystem function in the region. However, such products, often developed with the focus on upland landscapes, require additional testing and calibration for estuarine ecosystems.

Modeling Biomass and Carbon Stocks. In addition to biogeochemical fluxes, remote-sensing tools have also greatly advanced the modeling of vegetation biomass and carbon stocks in the challenging setting of estuarine emergent wetlands. Field spectroscopic measurements have been used to develop empirical relationships with above-ground plant biomass of Delta emergent freshwater marshes, and then scaled with three types of satellite data with contrasting resolutions (Byrd et al. 2014). In a later study, Byrd et al. (2018) developed a first-time remote-sensing-based model of the above-ground carbon stocks in tidal marshes for the whole conterminous United States, using San Francisco Bay as one of the regions for model calibration and relevant field sampling. The model was further used to generate spatially explicit predictions of tidal marsh biomass and percent carbon in tidal marsh plant tissue, thus demonstrating an important pathway towards cost-effective monitoring of coastal wetland blue carbon ecosystems (Byrd et al. 2018). Satellite imagery has also been used to model above-ground canopy properties relevant to photosynthetic functioning, such as proxies of canopy leaf area index. For example, Dronova and Taddeo (2016) reported a strong positive correlation between plant area index measured in tidal and impounded Suisun and West Delta

marshes and Landsat-based NDVI. However, this relationship was confounded by mixed pixels at the 30-m spatial resolution of satellite data and could not easily account for variation in canopy height (Dronova and Taddeo 2016). More generally, the challenges of mixed pixels and the limited sensitivity of passive sensors to canopy architecture increase the uncertainty in biomass and productivity modeling, and in applying the relationships established at well-measured sites to other regions.

These challenges highlight the need for more comprehensive and spatially explicit regional assessments of canopy structure, which can especially benefit from active remote-sensing tools, such as radar and LiDAR. One of the promising tools for regional applications is NASA's synthetic Uninhabited Aerial Vehicle Synthetic Aperture Radar (UAVSAR). UAVSAR delivers image products at high spatial resolution (varies by altitude but <10 m in many applications) and high temporal frequency that is pre-processed and openly distributed by the agency. Since the start of UAVSAR applications in 2008, the data have been collected through large parts of the state and most of the estuary (<https://uavsar.jpl.nasa.gov>), making it possible to systematically model and assess change. In a study of seasonal crop phenology in a portion of the Sacramento Valley within the Delta, H Li et al. (2019) reported sensitivity to different biomass stages in UAVSAR seasonal variability, which may be useful in modeling crop biophysical parameters, as shown by similar applications in other regions (e.g., Reisi-Gahrouei et al. 2019). Duncanson et al. (2020) applied both UAVSAR and airborne LiDAR data to model above-ground vegetation biomass in Sonoma County, California, including the northern portion of San Francisco Bay. The latter study reported biomass modeling challenges in tall, dense canopies because the signal couldn't penetrate them (Duncanson et al. 2020). An earlier LiDAR application by Rosso et al. (2006) reported similar challenges in characterizing the vegetation structure of tidal marshes in the San Francisco Bay because of the density of invasive cordgrass (*Spartina*). Although the latter study did not explicitly model biomass, it was able to detect

relevant changes in canopy height based on the difference in LiDAR-based digital surface models in consecutive years. However, overall, the high cost of acquiring data via LiDAR and the lack of systematic revisits has prevented widespread application of this instrumentation in modeling and monitoring primary productivity.

Another promising remote-sensing technology for high-spatial-resolution canopy structure data is structure-from-motion photogrammetry from UAVs. This technique uses overlapping images acquired from different perspectives to reconstruct a 3-D model of the landscape (Westoby et al. 2012). This technology has been demonstrated to be more accurate than LiDAR—comparable to survey-grade GPS (<3 cm)—in deriving fine-scale microtopography in tidal salt marshes on the New Brunswick coast (Kalacska et al. 2017). UAV-based structure from motion has also been demonstrated to be able to accurately estimate the height of salt marsh vegetation in North Carolina (DiGiacomo et al. 2020), and emergent macrophytes—including *Phragmites*, *Typha*, and *Scirpus*—in a freshwater wetland in Beijing (Jing et al. 2017). The latter study then successfully used the vegetation height data coupled with SVIs calculated from the spectral information in the ortho-image to estimate above-ground biomass. However, to our knowledge, applications of this technology have not yet been published for the estuary.

Notable progress has been also made in modeling below-ground biomass—an important component of primary productivity that is not directly visible to remote sensors. O’Connell et al. (2015) developed a hybrid modeling approach using proxies of foliar N and above-ground biomass from Landsat satellite data to predict below-ground biomass and root-to-shoot ratios for wetland species in the low-diversity freshwater impounded marshes in the West Delta (O’Connell et al. 2015). Inspiring examples of similar remote-sensing-based approaches have also been developed in other ecosystems, such as forest applications that use airborne hyperspectral remote-sensing tools (Madritch et al. 2014; Madritch et al. 2020), multispectral imagery

(Wicaksono et al. 2016) and LiDAR (Næsset and Gobakken 2008; Kristensen et al. 2015). Enhancing below-ground predictions is also becoming possible via more precise characteristics of 3-D canopy structure derived from the structure-from-motion UAV data (Lopatin et al. 2019). However, systematic protocols for modeling below-ground primary productivity based on such remote-sensing indicators across the diverse mosaic of regional ecosystems are still lacking.

Other Modeling Applications and Emerging Themes

Remote sensing of primary producers can greatly support several other ecological modeling initiatives in our region and other estuaries. Analyses of wildlife populations require spatially comprehensive proxies of habitat components and food resources, which often include vegetation. A relevant example of this is the modeling of avian abundance in northern San Francisco Bay and western Delta by Stralberg et al. (2010), which required both vegetation maps to identify habitats and SVIs as proxies of vegetation productivity derived from high-spatial-resolution aerial imagery (Stralberg et al. 2010). Importantly, habitat-related assessments of primary producers often require a high level of spatial detail to capture landscape elements related to fragmentation, connectivity, or signals of habitat change (Takekawa et al. 2012).

Regional efforts to model the effects of sea level rise (SLR) on estuarine environments have used remote-sensing products to characterize elevation; however, calibrating and validating such models may also require above- and below-ground biomass and productivity for dominant plant species, which field sampling has historically assessed (Stralberg et al. 2011; Schile et al. 2014). Studies from other geographic regions show the potential of remote sensing to assist in SLR modeling by providing satellite-derived proxies of wetland biomass density (Medeiros et al. 2015; Alizad et al. 2016); these proxies have been used to calibrate and validate or to map long-term changes in wetland types and land uses. (Wu et al. 2017). To produce robust and accurate outcomes, however, remote-sensing-based inputs to modeling SLR may need to reflect a high

level of ecological detail, i.e., identities of plant communities and their respective biophysical parameters.

Finally, there is a growing interest in remote-sensing-based indicators of biodiversity and particularly plant diversity (Pettorelli et al. 2016), which in earlier experimental field studies have shown strong positive relationships with vegetation biomass, primary productivity, and stability in the face of stressors (Schweiger et al. 2018). Although estuaries and other wetlands have been substantially under-studied in this regard compared to upland ecosystems, emerging evidence suggests the potential value of spectral and phenological remotely-sensed indicators of wetland plant diversity (Taddeo et al. 2019; Taddeo et al. 2021). Such indicators could also be of interest to monitoring programs that are expanding and seeking ways to detect early signals of biodiversity shifts in wetland restoration sites as well as in historical benchmark and reference ecosystems (WRMP 2020).

Data Quality Considerations

Integrating remote-sensing data sets into the modeling of primary-producer functions requires particular attention to data quality: both accurate mapping and reliable biophysical spectral indicators. For example, maps need to report how accurately they represent their categories, and, ideally, control for error when repeated over different time-steps. To minimize the effects of confounding factors such as variations in atmospheric conditions and sun angle, sophisticated atmospheric correction, image normalization, and other image pre-processing steps must be rigorous if SVIs are used as empirical biophysical indicators of ecosystem function (Samanta et al. 2010; Morton et al. 2014; Bi et al. 2016). Substantial field surveys are

always necessary to support the development of remote-sensing-based tools (Oikawa et al. 2017; Byrd et al. 2018; Dronova et al. 2021). However, field observations used to develop, calibrate, or validate the model need to be robust, and to statistically represent the target ecological characteristics.

Unaddressed errors and uncertainties are likely to propagate within modeling workflows, which can seriously impede long-term monitoring and change assessments. Furthermore, explicit assessments of resolution sensitivity and resolution-related uncertainty in modeling outcomes are extremely uncommon, presenting an important research need, given the growing variety of data products.

LOOKING AHEAD: THE VERY NEAR FUTURE OF REMOTE SENSING OF PRIMARY PRODUCERS IN THE ESTUARY

A Deluge of New Remote-Sensing Data

Orbital Hyperspectral Missions

Several recently launched (2018–2021) satellite-based remote instruments offer opportunities to advance the science and applications of primary productivity and should be more actively integrated in future monitoring and modeling. These include hyperspectral systems—EMIT (NASA), PRISMA (Italy), DESIS (Germany) and HISUI (Japan)—that provide repeated observations of high-spectral-resolution narrowband data relevant to detecting photosynthetic activity, plant stress, and primary production in the water column. Although the spatial resolution of orbital hyperspectral missions (~20 to 30 m, comparable to Landsat) can be considered somewhat coarse for mapping complex estuarine boundaries, the high spectral resolution could allow sub-pixel fractional estimations of different components—potentially at the species level—with existing well-established methodology (Li et al. 2005; Rosso et al. 2005; Hestir et al. 2008; Zomer et al. 2009; Ustin and Middleton 2021). Since the demise of NASA's Earth Observing Hyperion (EO-1) instrument, such capacity has been only available predominantly by expensive aerial imaging, and these new satellite sensors offer a breakthrough. Missions soon to be launched include the

Table 2 Select studies of remote sensing of primary producers in the San Francisco Estuary

Primary objective	Application focus	Data source	Study
Inventories and mapping of primary producers	Mapping aquatic vegetation	Airborne hyperspectral (HyMap) Airborne LiDAR	Khanna et al. 2011 Hestir et al. 2012
	Mapping wetland vegetation	Airborne hyperspectral (AVIRIS)	Li et al. 2005 Rosso et al. 2005 Zomer et al. 2009
		Multispectral satellite or aerial imaging	Zhang et al. 1997 Tuxen et al. 2008 Chapple and Dronova 2017
	Chlorophyll- <i>a</i> as indicator of water quality	Airborne hyperspectral (PRISM) <i>In situ</i> (optical sensors)	Fichot et al. 2016
	Invasive plant species: detection, mapping, monitoring change and invasion processes	Airborne hyperspectral	Underwood et al. 2003 Hestir et al. 2008 Khanna et al. 2012 Santos et al. 2016 Khanna et al. 2018
		UAV hyperspectral	Bolch et al. 2021
		Airborne hyperspectral Airborne LiDAR	Andrew and Ustin 2008
		Airborne <i>In situ</i> (Spectroscopy) Airborne LiDAR	Andrew and Ustin 2006 Santos et al. 2012 Rosso et al. 2006
Modeling biomass and structure of vegetation	Above-ground biomass (vegetation)	Satellite (Landsat) <i>In situ</i> (Spectroscopy)	Zhang et al. 1997
		Satellite (EO-1 Hyperion, Landsat, WorldView-2) <i>In situ</i> (Spectroscopy)	Byrd et al. 2014
		Satellite (Landsat) and Airborne (NAIP)	Byrd et al. 2018
		Airborne active sensors (UAVSAR, LiDAR)	H Li et al. 2019 Duncanson et al. 2020
	Below-ground biomass (vegetation)	Satellite (Landsat) <i>In situ</i> (Spectroscopy)	O'Connell et al. 2015
	Biomass of chlorophyll- <i>a</i> in water bodies	Aerial multispectral (Daedalus)	Catts et al. 1985
	Wetland canopy leaf area index	Satellite (Landsat) <i>In situ</i> (PhenoCam)	Dronova and Taddeo 2016 Oikawa et al. 2017
Modeling primary productivity and carbon fluxes	Modeling vegetation-controlled gross primary productivity (GPP) and net ecosystem exchange for CO ₂ (NEE)	<i>In situ</i> (Spectroscopy)	Matthes et al. 2015
	Parsing vegetation and water contributions to CH ₄ fluxes	Satellite (WorldView-2)	Matthes et al. 2014 Knox et al. 2017
	Predicting GPP in wetlands	Satellite (Landsat) <i>In situ</i> (PhenoCam)	Knox et al. 2017
Modeling properties of physical environment affecting primary production and influence of primary producers on the environment	Riparian ecosystem radiative transfer, shading, and water temperature	Airborne LiDAR	Greenberg et al. 2012
	The effects of landscape composition and vegetation types on phenology and ecosystem function	Satellite (Landsat, MODIS) Airborne hyperspectral	Andrew and Ustin 2009a Baldocchi et al. 2016 Anderson et al. 2018
	Habitat suitability of invasive wetland and riparian weeds	Airborne hyperspectral	Andrew and Ustin 2009b
	The effects of SAV on water column turbidity	Airborne hyperspectral <i>In situ</i> (Environmental Monitoring Program)	Hestir et al. 2016
Phenology of primary production	Seasonality of ecosystem function in restored wetlands	Satellite (Landsat, PlanetLabs) <i>In situ</i> (PhenoCam)	Dronova et al. 2021

German Aerospace Center EnMAP hyperspectral instrument, NASA's Surface Biology and Geology Mission, and the ESA's CHIME mission, which will—when coupled in a virtual constellation—provide 30-m hyperspectral data every 5 to 16 days, creating a Landsat-like data stream but with hyperspectral capabilities (Ustin and Middleton 2021).

Orbital Thermal Missions

Another highly relevant sensor is NASA's ECOSTRESS. Launched in 2018, ECOSTRESS offers thermal products that represent evapotranspiration, vegetation stress indicators, and land and water surface temperatures at an unprecedented spatial resolution of 30 to 70 m. Because the instrument is on board the International Space Station, the time of day the instrument passes over a specific site varies. Data collected over time enable characterization of the diurnal variability in surface temperature and derived estimates. Such data sets are critical for understanding local precursors of primary producer metabolism, which cannot be provided by thematic maps or simple greenness indices alone (Fisher et al. 2020). Recently, Halverson et al. (2021) and Gustine et al. (2021) demonstrated good performance of both Landsat and ECOSTRESS for measuring surface water temperature, with reasonable correlation to bulk temperature in the Delta, an important first step in advancing primary production modeling supported by remote sensing. In the context of our estuary, ECOSTRESS products also have promise in helping resolve uncertainties in characterizing vegetation biomass and productivity under variable tidal flooding, which could be manifested in thermal signatures of inundated communities.

Orbital LiDAR

Space-based LiDAR provides the hope of delivering critical missing puzzle pieces on productivity by systematically measuring ecosystem structure and biomass. The Global Ecosystem Dynamics Investigation (GEDI) mission launched at the end of 2018 for a 2-year global acquisition. The current design of this observation system is ill-suited for estuaries because it collects

data along small, spatially discrete footprints, and the continuous aggregated products have relatively coarse spatial resolution (25 m to 1 km). However, given the high demand for LiDAR products in assessments of vegetation canopy and topography (Buffington et al. 2016), this system provides an important relevant precedent for future satellite LiDAR missions and local applications of LiDAR on UAVs.

Wetland Hydrology

Hydrology is one of the primary determinants of wetland primary productivity. In 2023, NASA will launch NISAR, the NASA-Indian Space Research Organisation (ISRO) Synthetic Aperture Radar (SAR) mission. This will enable inundation mapping four to six times per month at a spatial resolution of 10 m, and highly precise water-level changes (~1 cm) every 6 days (Stavros et al. 2019). The capability to characterize hydrological fluxes in wetlands could enable improved modeling and monitoring of wetland primary productivity. Indeed, the recent launch of ESA's Sentinel-1 SAR mission has already demonstrated the value of space-based SAR for monitoring water level changes and soil moisture (Liao et al. 2020), soil organic carbon and bulk density (Yang and Guo 2019), and NEE modeling (Dabrowska-Zielinska et al. 2016) in various other wetland applications across the world.

Solar-Induced Fluorescence

Solar-induced fluorescence (SIF) has been shown to be an exceptionally good proxy for estimating photosynthesis, and thus providing a potentially more direct estimate of gross primary productivity from remote sensing for both terrestrial and aquatic ecosystems (Mohammed et al. 2019; Gupana et al. 2021). To date, only ocean color sensors with pixel sizes of 300 m to 1 km, and atmospheric satellite sensors with pixel sizes of 7 to 40 km, have the high spectral resolution or specific band position to detect SIF, making the application challenging for the estuary. However, down-scaling to improve spatial resolution is possible. Recently, Turner et al. (2020) down-scaled SIF measurements to a 500-m spatial resolution over California and showed reasonable agreement with GPP measured at the AmeriFlux

sites on Twitchell Island (R^2 ranged from 0.3 to 0.4).

Observing Carbon from Space

NASA's Orbiting Carbon Observatory (with the most recent mission, OCO-3, launched in 2019) monitors carbon dioxide in the Earth's atmosphere, with the potential to detect sinks and sources associated with land uses. However, its current spatial resolution of $\sim 3.5 \text{ km}^2$ —though high for global- and continental-level atmospheric monitoring—is overly coarse to adequately represent the regional mosaic of vegetation communities, land uses, and habitat types of estuarine ecosystems needed for management goals. More generally, efforts to integrate remote sensing with carbon monitoring, such as the CEOS Strategy for Carbon Observations from Space (CEOS 2014), still tend to emphasize “medium”- and “moderate”-resolution systems (30 m to 1000 m in the CEOS definition) that are well suited for upland terrestrial landscapes but limited for complex wetlands and other types of land–water interfaces. However, these initiatives increasingly recognize that policies will soon require much-higher-resolution spatially explicit products (CEOS 2014), which could stimulate further advances in remote-sensing technology and products.

Emerging Trends in Complementary Observation Technologies

A key prerequisite for success in remote-sensing-based assessments of primary producers is the ability to verify remote sensing-based inference with high-quality ground observations, which is a costly and logistically burdensome task in complex estuarine settings. Several field-data-collection initiatives, together with novel observation technologies, provide such opportunities in our region, and create incentives for more streamlined and collaborative data standardization and sharing.

Coordinated Vegetation Surveys

Relevant field data sets on primary producers include various vegetation survey efforts that collect data on plant coverage, species composition, and canopy structure via plot and transect sampling. Although data are not

commonly shared among individual projects now, several broader initiatives provide selected data sets via national and state repositories. For example, California Rapid Assessment Method (CRAM) collects rapid data on wetland conditions, which include several indicators of plant community composition and vertical structure (CRAM 2013). The National Wetland Condition Assessment program led by the USEPA in 2011 (USEPA 2016) collects vegetation composition, structure, and environmental characteristics across a nation-wide sample of wetland sites every 5 years. This program surveyed 26 sites in the estuary in the first survey in 2011, and 16 sites in the 2016 survey. Selected vegetation data sets for 2013 through 2016 are available from the monitoring of the National Estuarine Research Reserve (NERR) site via the agency's website. More locally, the Interagency Ecological Program (IEP) Aquatic Vegetation Project Working Team currently leads an initiative to publish a master aquatic vegetation data set for the Delta, compiled from past and ongoing monitoring and scientific programs across multiple state and federal agencies and universities. There is also a growing interest in more unified data-distribution platforms and repositories, making information available for different users. For example, the statewide California EcoAtlas portal uses a basemap from the California Aquatic Resource Inventory (CARI) to track the status of wetland projects' various databases, and already hosts some of the relevant assessments, such as CRAM sites.

The Nets: AeroNet, FluxNet, SpecNET, and PhenoCamNet

Because the atmosphere's effects are arguably the largest source of uncertainty in chlorophyll-*a* retrieval from the water column (up to 90%), uncertainty about water-leaving radiance and reflectance must be rigorously quantified and its correction validated as a best practice for remote sensing of primary producers in the water column (Salama and Stein 2009; Gilerson et al. 2022). The Aerosol Robotic NETwork Ocean Color (AERONET-OC) network of autonomous radiometer systems, which are globally distributed at fixed offshore and coastal sites, are critical infrastructure in validating and verifying the atmospheric

correction for water-leaving radiances and remote-sensing reflectance products for water-column studies (Zibordi et al. 2009). The recent installation of an AERONET-OC site in Grizzly Bay provides an emerging opportunity to verify and improve atmospheric correction specifically for the estuary's conditions.

Among direct measurements of ecosystem productivity, publicly available products are available from the AmeriFlux network of sites that measure fluxes of carbon, water, and energy across the US (Baldocchi et al. 2001). The San Francisco Estuary region contains 18 AmeriFlux stations, many of which are currently active and provide publicly accessible measurements of ecosystem fluxes in CO₂, CH₄, water vapor, and a suite of relevant environmental variables across different representative ecosystems: different-aged tidal and freshwater marshes (including the newer subsidence reversal projects), pastureland, and common crop types that are seen as important alternative land uses in the Delta (Matthes et al. 2015; Knox et al. 2016; Hemes et al. 2019). Some of these sites are equipped with PhenoCams that are well suited for (1) assessing vegetation composition, (2) how annual budgets of carbon uptake are functioning, (3) phenological patterns, and (4) broader-scale effects of restored wetlands and flooded agriculture on subregional microclimates and ecosystem functioning (Baldocchi et al. 2016). A wider adoption of cost-effective PhenoCams across the region, and integration with the broader continental-scale PhenoCam cooperative network, would be highly promising to systematically monitor ecological seasonality much less invasively than field surveys.

Most common applications of PhenoCams to date use their imagery to compute SVIs of greenness from local vegetation that the sensors observe. However, advances in automated photo recognition and interpretation could make it possible to extract other relevant data from the time-lapse images, such as the flooding, flowering, and fruiting cycles of plant species; disturbance; wildlife uses; and more. Combining PhenoCams with other *in*

situ sensors that measure meteorological, edaphic, and hydrological conditions thus offers a powerful strategy for more comprehensive data acquisition to investigate local drivers of primary productivity, to validate satellite-based assessments, and to facilitate up-scaling for carbon budgeting at the regional level.

The American SpecNet and new ChinaSpec Network of *in situ* optical instruments co-located with eddy-covariance towers provide a promising model for long-term, ground-based measurements of SIF, SVIs and other indicators of biodiversity—a model which could be used to further advance remote sensing of primary productivity, were such instruments to be deployed in the estuary (Gamon 2015; Zhang et al. 2021).

High-Frequency and High-Throughput In Situ Optical Sensors

In situ optical instruments can rapidly make proxy measurements of water-column hyperspectral absorption, attenuation and backscatter, chlorophyll-*a* and other phytoplankton pigments, dissolved organic matter, nutrients, and other abiotic conditions of the water column at very high temporal resolution (seconds to minutes) (Saraceno et al. 2009; Pellerin 2015). When mounted on boats with a continuous pumping system and GPS integration, such instruments provide spatially contiguous *in situ* aquatic biogeochemical data that can be used for monitoring, modeling, and remote-sensing calibration and validation (Fichot et al. 2016).

NASA Airborne Radiometry for Coastal and Inland Waters

Over the past decade, NASA has tested several airborne mission concepts to collect rigorous atmospheric and aquatic radiometric measurements over inland and coastal water bodies of California, including Monterey Bay, Lake Tahoe, and San Francisco Bay. Although not an imaging system, the instrument suite provides high-spectral-resolution and high-fidelity measurements, which—when geo-located with *in situ* radiometry and satellite imaging—can provide science-quality data to calibrate and validate next-generation NASA missions, and thus provide higher-accuracy local products for the estuary

community (agency managers, scientists, and other stakeholders, etc.) (Guild et al. 2020)

Participatory Science

The growing participatory science effort also offers interesting opportunities to fill spatial gaps in understanding primary producers and ecosystem characteristics that can help inform mapping and validation, even though the detail and sampling quality of data may differ from systematically designed research surveys. The large global iNaturalist database (<https://www.inaturalist.org/>) collects geolocated public reports on many biological species, including plants. Various initiatives that invite public reports and monitoring of native and invasive plant species are led by the California Native Plant Society and the CDFW (such as the EDDMapS mobile application to report sightings of invasive species). The USA-NPN's (National Phenology Network's) database is also accumulating observations of plant and animal seasonality from a wide pool of public participants via a program "Nature's Notebook" that supports online submissions of phenological observations and development by the participants of locally focused phenology programs (https://www.usanpn.org/natures_notebook). While such efforts in the estuary have predominantly concentrated on "emergent" vegetation components, notable examples of initiatives that focus on aquatic domains could be extended to the estuary. A great example of this is the NASA-funded project Floating Forest that focuses on the dynamics of global marine kelp forests and engages public participation via the Zooniverse platform (<https://www.zooniverse.org/projects/zooniverse/floating-forests/about/research>).

Data Access and Discovery

There are an ever-increasing number of analysis-ready data products available for download by users from agencies such as the USGS, NASA, NOAA, and the ESA. These include surface reflectance products that eliminate the need for atmospheric correction, and derived products including NDVI, EVI, LAI, phenology, land cover, NPP, GPP, and more. These products are often developed to be reasonably accurate at the global or continental scale, but are often ill-

sued for the precise, local solutions needed to support management decisions in the estuary. Compounding this challenge is the new reality that open-access data are now everywhere but are often not easily discoverable. Users must navigate multiple different data portals to discover what products are available to them. Even within NASA, multiple different distributed active archive data centers (DAACS) process, archive, document, and distribute data, including Land Processes, Physical Oceanography, National Snow and Ice Data Center, and many more. Recent advances are helping users overcome these challenges, such as the Data Pathfinders in NASA's Earthdata website that provide direct links to commonly used data sets, curated by scientific application area. New cloud-based data processing and sharing interfaces such as Google Earth Engine, the CSIRO Data Cubes, and the USGS's ScienceBase further facilitate data sharing and reduce the need to download and store large, publicly available data sets. With the emergence of such tools and platforms arises an opportunity to help managers and researchers close the loop between remote sensing and decision-making.

Preparing for the Very Near Future?

Research Priorities

Maximizing the potential of remote sensing to support modeling primary producers and their functions require more informed guidance to choose sensors, primary-producer indicators, and application scales for a given management problem. Maximizing remote sensing's potential demands more comparative studies across different types of data, resolutions, and indicators. Developing such guidance in a unique estuarine context requires overcoming the unique barriers of land-water interfaces, such as high spatial heterogeneity and spectral artifacts that result from the hydrological attenuation of plant signals (Kearney et al. 2009), obstruction of reflectance or backscattering by dense canopies (Rosso et al. 2006; Duncanson et al. 2020), and adjacency effects caused by light being scattered from nearby terrestrial surfaces to aquatic targets (Mouw et al. 2015). Advances in highly customizable, locally applicable remote

sensors—such as PhenoCams and UAVs (Knox et al. 2017; Coops et al. 2019; Bolch et al. 2021)—offer new timely and cost-effective opportunities for navigating these challenges, given the infamous constraints on field surveys in wetland and coastal settings.

On the application side, a notable gap still exists on the connections between “land” and “water” domains that historically have been approached by different disciplinary fields. Truly advancing the capacity to model and monitor primary productivity requires a more seamless integration of the contributing processes across land–water interfaces as well as accounting for their unique synergies and feedbacks. Earlier studies in the region provide insightful examples of such feedbacks; for example, Greenberg et al. (2012) showed that changes in radiative transfer in riparian zones may have implications for the growth and productivity of SAV. Phenological contrasts in reed-dominated canopies of novel impounded marshes show important associations with water temperature, microclimate, and the timing of whole-ecosystem primary productivity and greenhouse gas fluxes (Eichelmann et al. 2018; Dronova et al. 2021). Limited understanding of such feedback points to larger uncertainties about how wetland transitional zones respond to the combined effects of warming temperatures, SLR, and changing salinity patterns (Callaway and Parker 2012; Beagle et al. 2019). The unprecedented monitoring capacity that modern remote-sensing platforms offer should be explored as a critical step toward resolving these uncertainties.

Closing the Loop Between Data and Management Decisions

The techniques and applicability of remote sensing to advance the scientific study of primary producers in the Delta are well developed, and clearly there are many management-relevant applications and products. Traditional barriers to the access and use of satellite data are disappearing. Yet, there is still a gap between map generation and management decisions. Ongoing challenges include the need for regionally specific, accurate data products that

include well-quantified and well-communicated uncertainties, benchmarked against the existing data sets used to inform decisions (Sheffield et al. 2018). Additionally, challenges associated with continuity and data latency remain. As discussed above, there is no systematic monitoring mandate for airborne remote-sensing data collection, yet the value of annual hyperspectral remote sensing in the Delta has been repeatedly demonstrated. University researchers who produce many of the innovative products useful for informing management do not have the mandate, scope, or funding to produce products operationally beyond the research phase, and federal agencies charged with such operations (e.g., NASA, NOAA) do not provide the regionally-tuned products necessary for location-specific management decisions. Integrated environmental data analysis and visualization tools for synthesis and readily accessible online portals targeted to local needs could improve regional data-driven decision-making (McCarthy et al. 2017).

Collaboration Across Management Goals

Evidence from diverse remote-sensing applications in the region underscores the critical need for collaborations across different management goals. Primary producers play a unique role that unifies a wide range of ecological questions—from biogeochemistry to food webs—and this versatility can be an important focal point in holistic policy, planning, and monitoring initiatives. Recognizing this versatility makes it obvious that using remote-sensing applications to map and model primary producers can benefit efforts well beyond immediate target projects. Similarly, local, *in situ* data sets on primary producers can benefit regional-scale efforts by providing monitoring baselines and opportunities to calibrate and validate primary productivity models at landscape scales.

This calls for more communication and sharing of information. For example, the DSC’s Delta Science Program Remote Imaging Collaborative initiative aims to leverage various remote-sensing data sets and research efforts to promote communication as well as data and methodology sharing among Delta geospatial researchers and

data users. Important initiatives are also arising to streamline, consolidate, and enhance the capacity to monitor wetlands by using both field- and remote-sensing-based indicators. A notable example is the Wetland Regional Monitoring Program coordinated by the San Francisco Estuary Partnership (WRMP 2020), which is developing wetland indicators in response to pertinent guiding management questions concerning both the status and future dynamics of wetland projects. WRMP's comprehensive scope recognizes both the unique potential of remote-sensing tools to support cost-effective spatio-temporal indicators and the need to integrate them with field-based calibration and validation (WRMP 2020).

The time is especially ripe to develop such coordinated efforts in the light of the state's efforts to integrate carbon- and biodiversity-related goals in frameworks such as nature-based carbon solutions (Wedding et al. 2021) and in the convergence of other related initiatives that must leverage remotely-sensed data to realize their stated goals. From the ecological perspective, such efforts raise critical questions about where carbon and biodiversity goals can be well aligned (i.e., ecosystems and management pathways where higher diversity is expected to increase productivity) or not (low-diversity systems with high carbon sequestration potential or, in contrast, important high-biodiversity systems with low productivity) and how to best support synergistic measures and adaptive management action portfolios. Ultimately, these considerations are critical both to reconcile economic and ecological priorities as well as to balance the different priorities of stakeholders who manage ecosystems. (Deverel et al. 2017; DSC 2019; Chamberlin et al. 2020).

Capacity Building

Developing the workforce is critical to preparing the current and next generation of researchers and managers to take advantage of the oncoming data deluge. They must be conversant in data science and possess the computational skills to perform cloud computing and develop and execute code across multiple platforms. Many

analysis tools also come with plentiful outreach materials. Google provides a whole suite of online training materials for Google Earth Engine and graphics processing unit (GPU)-enabled machine learning (Google Colaboratory), with the user community contributing many more. The National Science Foundation's National Ecological Observatory Network (NEON) provides online training materials for the analysis of airborne hyperspectral and LiDAR data, with a focus on open-source R and Python. NASA's Applied Remote Sensing Training (ARSET) provides online and in-person training to beginning through advanced practitioners to use satellite remote sensing in their environmental management and decision-making across NASA's Applied Science focal areas of Land, Water Resources, Disasters, and Health and Air Quality. However, the workforce must also be equipped with the domain knowledge to appreciate the ecological underpinnings of the estuary and view remote-sensing technologies with the critical lens that all measurement technologies and data sources warrant.

The role of the University of California (UC) and California State University (CSU) is critical in this endeavor, as stewards of education, research, and workforce development for the state of California. An excellent model of this is the UC Agriculture and Natural Resources Drone Camp: collaborative efforts between several UC and CSU campuses that provide an intensive short course for participants who want to learn drone mapping. Workforce development also includes the future workforce, which must start with inspiration, and focus on retention, with a particular eye toward diversifying the workforce. This requires engagement with K-14 students and investment in student and early-career research. The California Sea Grant and Delta Science Program fellowships provide an excellent model from which to build for recent graduates.

Capacity building also includes strengthening and integrating new and different areas of science. Remote-sensing technology and its applications must be co-developed so that its engineering requirements are integrated with the needs of

scientific investigations; then meaningful results can be delivered to managers and decision-makers. Remote-sensing products need to be generated and delivered in a way that can be used by more managers and stakeholders in the Delta, and feedback mechanisms need to be developed that can feed local knowledge into improving the accuracy of remote-sensing products to meet local needs.

Remote sensing is not a panacea to meet all monitoring needs; it is a complement to other measurement techniques and technologies. *In situ* measurements are critical to calibration and validation of remote-sensing algorithms, quantifying the uncertainty in remote-sensing maps, and for modeling biomass and carbon stocks. Thus, investments that maintain and build capacity for *in situ* measurements should continue, with an eye toward improving their complementarity with remote sensing whenever possible. When possible, design of plot sizes, sample size, and distribution should include consideration of remote-sensing resolution, and the timing of collection should consider remote-sensing platform overpasses and optimal phenological stage for remote-sensing detection. Complementarity also includes collecting and reporting spatial data quality and metadata, including attribute accuracy, positional accuracy, temporal accuracy, logical consistency, completeness, and lineage (Reinke and Jones 2006).

Finally, infrastructure is a critical and often overlooked component of capacity building. Recent attention has been paid to the aging physical infrastructure of California with a particular focus on climate resiliency, as highlighted in the 2021 Five-Year Infrastructure Plan. What is missing from this and most long-term plans is the physical-cyber infrastructure needed to support the growing data needs that remote sensing poses. For example, The Open and Transparent Water Data Act (AB 1755) requires the CDWR to create, operate and maintain a statewide water data platform that integrates water and ecological data and requires all state-funded grant recipients to adhere to protocols for data sharing, documentation, and public access.

Yet, no state agency has defined these protocols, nor does any individual agency have the financial resources or physical-cyber infrastructure to house and serve the terabytes and petabytes of raster data generated from remote-sensing analyses. Commercial cloud services are a viable alternative to creating new cyber infrastructure for the state but require ongoing an ongoing and relatively high-cost investment to maintain the service if the data must be 'hot' for frequent analyses and access. Infrastructure cannot be built or maintained without investment; this funding should be a priority at local, state, and federal levels.

CONCLUSIONS

- Remote-sensing imagery is an effective tool to complement monitoring the distribution and biomass of primary producers as well as modeling primary productivity in the Delta across the full environmental gradient: from the water column to wetland and terrestrial environments.
- The effectiveness of remote sensing in primary-producer assessments depends on its particular application to a management need and must be considered in the context of trade-offs in spatial, temporal, spectral, and radiometric scales of both the image data and the ecological targets and processes of interest.
- Maximizing the benefits offered by the growing deluge of open and accessible new sensor data—including UAV imaging, space-based imaging spectroscopy, dual-band SAR, and LiDAR—to meet regional needs requires greater capacity-building for people and institutions, greater cooperation between research groups, and standardization of large-data-file management and sharing to meet user needs and legislated requirements (e.g., AB 1755).

ACKNOWLEDGEMENTS

The authors would like to thank Drs. Clifford Dahm, Louise Conrad and Sam Bashevkin of the Delta Stewardship Council for providing reviews and feedback on the conceptualization and early drafts of this manuscript. We also wish to thank Jacob Nesslage, Vincent Pascual, Erik Bolch, and Dr. Shruti Khanna for contributing figures and data for figures. Finally, we would like to acknowledge the two anonymous peer reviewers of this manuscript, for doing the unsung and under-appreciated labor that is so critical to maintaining the integrity of science and scholarly communication. We thank them for their service.

REFERENCES

- Adam E, Mutanga O, Rugege D. 2010. Multispectral and hyperspectral remote sensing for identification and mapping of wetland vegetation: a review. *Wetl Ecol Manag.* [accessed 2022 Oct 14];18(3):281–296. <https://doi.org/10.1007/s11273-009-9169-z>
- Ade C, Hestir EL, Khanna S, Ustin SL. 2022. Genus-level mapping of invasive floating aquatic vegetation using Sentinel-2 satellite remote sensing. *Remote Sens.* [accessed 2022 Oct 14];14(13):3013. <https://doi.org/10.3390/rs14133013>
- Ade C, Hestir EL, Lee CM. 2021. Assessing fish habitat and the effects of an emergency drought barrier on estuarine turbidity using satellite remote sensing. *J Am Water Res Assoc.* [accessed 2022 Oct 14];57(5):752–770. <https://doi.org/10.1111/1752-1688.12925>
- Alizad K, Hagen SC, Morris JT, Medeiros SC, Bilskie M v, Weishampel JF. 2016. Coastal wetland response to sea-level rise in a fluvial estuarine system. *Earth's Future.* [accessed 2022 Oct 14];4(11):483–497. <https://doi.org/10.1002/2016EF000385>
- Anderson FE, Bergamaschi B, Sturtevant C, Knox S, Hastings L, Windham–Myers L, Detto M, Hestir EL, Drexler J, Miller RL, et al. 2016. Variation of energy and carbon fluxes from a restored temperate freshwater wetland and implications for carbon market verification protocols: variability in wetland fluxes. *J Geophys Res: Biogeosci.* [accessed 2022 Oct 14];121(3):777–795. <https://doi.org/10.1002/2015JG003083>
- Anderson M, Gao F, Knipper K, Hain C, Dulaney W, Baldocchi D, Eichelmann E, Hemes K, Yang Y, Medellin–Azuara J, et al. 2018. Field-scale assessment of land and water use change over the California Delta using remote sensing. *Remote Sensing.* [accessed 2022 Oct 14];10(6):889. <https://doi.org/10.3390/rs10060889>
- Andrew ME, Ustin SL. 2006. Spectral and physiological uniqueness of perennial Pepperweed (*Lepidium latifolium*). *Weed Sci.* [accessed 2022 Oct 14];54(6):1051–1062. <http://www.jstor.org/stable/4539505>
- Andrew ME, Ustin SL. 2008. The role of environmental context in mapping invasive plants with hyperspectral image data. *Remote Sens Environ.* [accessed 2022 Oct 14];112(12):4301–4317. <https://doi.org/10.1016/j.rse.2008.07.016>
- Andrew ME, Ustin SL. 2009a. Effects of microtopography and hydrology on phenology of an invasive herb. *Ecography.* [accessed 2022 Oct 14];32(5):860–870. <https://doi.org/10.1111/j.1600-0587.2009.05930.x>
- Andrew ME, Ustin SL. 2009b. Habitat suitability modelling of an invasive plant with advanced remote sensing data. *Divers Distrib.* [accessed 2022 Oct 14];15(4):627–640. <https://doi.org/10.1111/j.1472-4642.2009.00568.x>
- Baldocchi D, Falge E, Gu LH, Olson R, Hollinger D, Running S, Anthoni P, Bernhofer C, Davis K, Evans R, et al. 2001. FLUXNET: a new tool to study the temporal and spatial variability of ecosystem-scale carbon dioxide, water vapor, and energy flux densities. *Bul Am Meteorol Soc.* [accessed 2022 Oct 14];82(11):2415–2434. [https://doi.org/10.1175/1520-0477\(2001\)082<2415:FAN TTS>2.3.CO;2](https://doi.org/10.1175/1520-0477(2001)082<2415:FAN TTS>2.3.CO;2)
- Baldocchi D, Knox S, Dronova I, Verfaillie J, Oikawa P, Sturtevant C, Matthes JH, Detto M. 2016. The impact of expanding flooded land area on the annual evaporation of rice. *Agric For Meteorol.* [accessed 2022 Oct 14];223:181–193. <https://doi.org/10.1016/j.agrformet.2016.04.001>
- Balsamo G, Agusti–Panareda A, Albergel C, Arduini G, Beljaars A, Bidlot J, Blyth E, Bousserez N, Boussetta S, Brown A, et al. 2018. Satellite and *in situ* observations for advancing global earth surface modelling: a review. *Remote Sens.* [accessed 2022 Oct 14];10(12):2038. <https://doi.org/10.3390/rs10122038>

- Beagle J, Lowe J, McKnight K, Safran S, Tam L, Szambelan S, Jo S. 2019. San Francisco Bay shoreline adaptation atlas: working with nature to plan for sea level rise using Operational Landscape Units. SFEI Contribution No. 915. Richmond (CA): San Francisco estuary Institute & San Francisco Bay Area Planning and Urban Research Association (SPUR). [accessed 2022 Oct 14]; 255 p. Available from: <https://www.sfei.org/documents/adaptationatlas>
- Bekaert DPS, Jones CE, An K, Huang M–H. 2019. Exploiting UAVSAR for a comprehensive analysis of subsidence in the Sacramento Delta. *Remote Sens Environ.* [accessed 2022 Oct 14];220:124–134. <https://doi.org/10.1016/j.rse.2018.10.023>
- Bi J, Myneni R, Lyapustin A, Wang Y, Park T, Chi C, Yan K, Knyazikhin Y. 2016. Amazon forests' response to droughts: a perspective from the MAIAC product. *Remote Sens.* [accessed 2022 Oct 14];8(4): 356. <https://doi.org/10.3390/rs8040356>
- Bolch EA, Hestir EL, Khanna S. 2021. Performance and feasibility of drone-mounted imaging spectroscopy for invasive aquatic vegetation detection. *Remote Sensing.* [accessed 2022 Oct 14];13(4): 582. <https://doi.org/10.3390/rs13040582>
- Bolch EA, Santos MJ, Ade C, Khanna S, Basinger NT, Reader MO, Hestir EL. 2020. Remote detection of invasive alien species. In: Cavender–Bares J, Gamon JA, Townsend PA (editors). *Remote sensing of plant biodiversity*. Cham: Springer International Publishing. [accessed 2022 Oct 14]; p 267–307. https://doi.org/10.1007/978-3-030-33157-3_12
- Bolton DK, Gray JM, Melaas EK, Moon M, Eklundh L, Friedl MA. 2020. Continental-scale land surface phenology from harmonized Landsat 8 and Sentinel-2 imagery. *Remote Sens Environ.* [accessed 2022 Oct 14];240:111685. <https://doi.org/10.1016/j.rse.2020.111685>
- Boul R, Keeler–Wolf T. 2016. 2012 vegetation map update for Suisun Marsh, Solano County, California: a report to the California Department of Water Resources. [accessed 2022 Oct 14];74 p. Available from: <http://nrm.dfg.ca.gov/FileHandler.ashx?DocumentID=123411>
- Boyer K, Sutula M. 2015. Factors controlling submersed and floating macrophytes in the Sacramento–San Joaquin Delta. Costa Mesa (CA): Southern California Coastal Water Research Project. SCCWRP Technical Report 870. [accessed 2022 Oct 14];97 p. Available from: https://ftp.sccwrp.org/pub/download/DOCUMENTS/TechnicalReports/870_FactorsControllingSubmersedAndFloatingMacrophytesInSac-SanJoaquinDelta.pdf
- Bracher A, Bouman HA, Brewin RJW, Bricaud A, Brotas V, Ciotti AM, Clementson L, Devred E, di Cicco A, Dutkiewicz S, et al. 2017. Obtaining phytoplankton diversity from ocean color: a scientific roadmap for future development. *Front Mar Sci.* [accessed 2022 Oct 14];4:55. <https://doi.org/10.3389/fmars.2017.00055>
- Brewin RJW, Sathyendranath S, Platt T, Bouman H, Ciavatta S, Dall'Olmo G, Dingle J, Groom S, Jönsson B, Kostadinov TS, et al. 2021. Sensing the ocean biological carbon pump from space: A review of capabilities, concepts, research gaps and future developments. *Earth–Sci Rev.* [accessed 2022 Oct 14];217:103604. <https://doi.org/10.1016/j.earscirev.2021.103604>
- Brisco B. 2015. Mapping and monitoring surface water and wetlands with synthetic aperture radar. In: Tiner RW, Lang MW, Klemas VV (editors). *Remote sensing of wetlands*. Boca Raton (FL): CRC Press. [accessed 2022 Oct 14]. p 119–136. <https://doi.org/10.1201/b18210>
- Buffington KJ, Dugger BD, Thorne KM, Takekawa JY. 2016. Statistical correction of lidar-derived digital elevation models with multispectral airborne imagery in tidal marshes. *Remote Sens Environ.* [accessed 2022 Oct 14];186:616–625. <https://doi.org/10.1016/j.rse.2016.09.020>
- Byrd KB, Ballanti L, Thomas N, Nguyen D, Holmquist JR, Simard M, Windham–Myers L. 2018. A remote sensing-based model of tidal marsh aboveground carbon stocks for the conterminous United States. *ISPRS J Photogram Remote Sens.* [accessed 2022 Oct 14];139:255–271. <https://doi.org/10.1016/j.isprsjprs.2018.03.019>
- Byrd KB, O'Connell JL, di Tommaso S, Kelly M. 2014. Evaluation of sensor types and environmental controls on mapping biomass of coastal marsh emergent vegetation. *Remote Sens Environ.* [accessed 2022 Oct 14];149:166–180. <https://doi.org/10.1016/j.rse.2014.04.003>

- Callaway JC, Parker VT. 2012. Current issues in tidal marsh restoration. In: Palaima A (editor). Ecology, conservation, and restoration of tidal marshes: the San Francisco estuary. Berkeley (CA): University of California Press. [accessed 2022 Oct 14]; p 253–262. <https://doi.org/10.1525/california/9780520274297.003.0018>
- Catts GP, Khorram S, Cloern JE, Knight AW, Degloria SD. 1985. Remote sensing of tidal chlorophyll a variations in estuaries. *Intl J Remote Sens.* [accessed 2022 Oct 14];6(11):1685–1706. <https://doi.org/10.1080/01431168508948318>
- [CDFA] California Department of Food and Agriculture 2020. California Agricultural Statistics Review 2020–2021. Sacramento (CA): CDFA [accessed 2022 Oct 14]. 156 p. Available from: https://www.cdfa.ca.gov/Statistics/PDFs/2021_Ag_Stats_Review.pdf
- [CDFW] California Department of Fish and Wildlife 2020. Survey of California Vegetation Classification and Mapping Standards. Sacramento (CA): CDFW. [accessed 2022 Oct 14]. Available from: <https://nrm.dfg.ca.gov/FileHandler.ashx?DocumentID=102342>
- [CEOS] The Committee on Earth Observation Satellites. 2014. CEOS strategy for carbon observations from space: the Committee on Earth Observation Satellites (CEOS) response to the Group on Earth Observations (GEO) carbon strategy. [accessed 2022 Oct 14]. 216 p. Japan: JAXA, I&A Corporation. Available from: https://ceos.org/document_management/Publications/WGClimate_CEOS-Strategy-for-Carbon-Observations-from-Space_Apr2014.pdf
- Chamberlin S, Passero M, Conrad–Saydah A, Biswas T, Stanley CK. 2020. Nature-based climate solutions: a roadmap to accelerate action in California. The Nature Conservancy. [accessed 2022 Oct 14]. 113 p. Arlington (VA): The Nature Conservancy. Available from: https://www.nature.org/content/dam/tnc/nature/en/documents/TNC_Pathways_2020vf.pdf
- Chapple D, Dronova I. 2017. Vegetation development in a tidal marsh restoration project during a historic drought: a remote sensing approach. *Front Mar Sci.* [accessed 2022 Oct 14];4:243. <https://doi.org/10.3389/fmars.2017.00243>
- Ciriello V, Lee J, Tartakovsky DM. 2021. Advances in uncertainty quantification for water resources applications. *Stoch Environ Res Risk Asses.* [accessed 2022 Oct 14];35(5):955–957. <https://doi.org/10.1007/s00477-021-01998-y>
- Clark ML. 2017. Comparison of simulated hyperspectral HypsIRI and multispectral Landsat 8 and Sentinel-2 imagery for multi-seasonal, regional land-cover mapping. *Remote Sens Environ.* [accessed 2022 Oct 14];200:311–325. <https://doi.org/10.1016/j.rse.2017.08.028>
- Claverie M, Ju J, Masek JG, Dungan JL, Vermote EF, Roger J–C, Skakun SV, Justice C. 2018. The harmonized Landsat and Sentinel-2 surface reflectance data set. *Remote Sens Environ.* [accessed 2022 Oct 14];219:145–161. <https://doi.org/10.1016/j.rse.2018.09.002>
- Conrad JL, Bibian AJ, Weinersmith KL, de Carion D, Young MJ, Crain P, Hestir EL, Santos MJ, Sih A. 2016. Novel species interactions in a highly modified estuary: association of Largemouth Bass with Brazilian Waterweed *Egeria densa*. *Trans Am Fish Soc.* [accessed 2022 Oct 14];145:249–263. <https://doi.org/10.1080/00028487.2015.1114521>
- Coops NC, Goodbody TRH, Cao L. 2019. Four steps to extend drone use in research. *Nature.* [accessed 2022 Oct 14];572(7770):433–435. <https://doi.org/10.1038/d41586-019-02474-y>
- [CRAM] California Rapid Assessment Method for wetlands 2013. 2013. [accessed 2022 Oct 14]. Available from: <https://www.cramwetlands.org/documents?title=wetlands>
- Dabrowska–Zielinska K, Budzynska M, Tomaszewska M, Malinska A, Gatkowska M, Bartold M, Malek I. 2016. Assessment of carbon flux and soil moisture in wetlands applying Sentinel-1 Data. *Remote Sens.* [accessed 2022 Oct 14];8(9). <https://doi.org/10.3390/rs8090756>
- Deverel S, Jacobs P, Lucero C, Dore S, Kelsey TR. 2017. Implications for greenhouse gas emission reductions and economics of a changing agricultural mosaic in the Sacramento–San Joaquin Delta. *San Franc estuary Watershed Sci.* [accessed 2022 Oct 14];15(3). <https://doi.org/10.15447/sfews.2017v15iss3art2>

- Dierssen H, McManus GB, Chlus A, Qiu D, Gao B–C, Lin S. 2015. Space station image captures a red tide ciliate bloom at high spectral and spatial resolution. *Proc Natl Acad Sci USA*. [accessed 2022 Oct 14];112(48):14783–14787. <https://doi.org/10.1073/pnas.1512538112>
- Dierssen HM, Ackleson SG, Joyce KE, Hestir EL, Castagna A, Lavender S, McManus MA. 2021. Living up to the hype of hyperspectral aquatic remote sensing: science, resources and outlook. *Front Environ Sci*. [accessed 2022 Oct 14];9:134. <https://doi.org/10.3389/fenvs.2021.649528>
- DiGiacomo AE, Bird CN, Pan VG, Dobroski K, Atkins–Davis C, Johnston DW, Ridge JT. 2020. Modeling salt marsh vegetation height using unoccupied aircraft systems and structure from motion. *Remote Sens*. [accessed 2022 Oct 14];12(14). <https://doi.org/10.3390/rs12142333>
- Downing BD, Bergamaschi BA, Kraus TEC. 2017. Synthesis of data from high-frequency nutrient and associated biogeochemical monitoring for the Sacramento–San Joaquin Delta, northern California. United States Geological Survey Scientific Investigations Report 2017-5066. Reston (VA): USGS. [accessed 2022 Oct 14];28 p. <https://doi.org/10.3133/sir20175066>
- Dronova I, Gong P, Clinton NE, Wang L, Fu W, Qi S, Liu Y. 2012. Landscape analysis of wetland plant functional types: the effects of image segmentation scale, vegetation classes and classification methods. *Remote Sens Environ*. [accessed 2022 Oct 14];127:357–369. <https://doi.org/10.1016/j.rse.2012.09.018>
- Dronova I, Taddeo S. 2016. Canopy leaf area index in non-forested marshes of the California Delta. *Wetlands*. [accessed 2022 Oct 14];36(4):705–716. <https://doi.org/10.1007/s13157-016-0780-5>
- Dronova I, Taddeo S, Hemes KS, Knox SH, Valach A, Oikawa PY, Kasak K, Baldocchi DD. 2021. Remotely sensed phenological heterogeneity of restored wetlands: linking vegetation structure and function. *Agric For Meteorol*. [accessed 2022 Oct 14];296:108215. <https://doi.org/10.1016/j.agrformet.2020.108215>
- [DSC] Delta Stewardship Council. 2019. The Delta Plan (as amended in 2019). [accessed 2022 Oct 14]. Sacramento (CA): DSC. Available from: <https://www.deltacouncil.ca.gov/delta-plan/>
- Duncanson L, Neuenschwander A, Hancock S, Thomas N, Fatoyinbo T, Simard M, Silva CA, Armston J, Luthcke SB, Hofton M, et al. 2020. Biomass estimation from simulated GEDI, ICESat-2 and NISAR across environmental gradients in Sonoma County, California. *Remote Sens Environ*. [accessed 2022 Oct 14];242:111779. <https://doi.org/10.1016/j.rse.2020.111779>
- Eichelmann E, Hemes KS, Knox SH, Oikawa PY, Chamberlain SD, Sturtevant C, Verfaillie J, Baldocchi DD. 2018. The effect of land cover type and structure on evapotranspiration from agricultural and wetland sites in the Sacramento–San Joaquin River Delta, California. *Agric For Meteorol*. [accessed 2022 Oct 14];256–257:179–195. <https://doi.org/10.1016/j.agrformet.2018.03.007>
- Fichot CG, Downing BD, Bergamaschi BA, Windham–Myers L, Marvin–DiPasquale M, Thompson DR, Gierach MM. 2016. High-resolution remote sensing of water quality in the San Francisco Bay–Delta estuary. *Environ Sci Technol*. [accessed 2022 Oct 14];50(2):573–583. <https://doi.org/10.1021/acs.est.5b03518>
- Fisher JB, Lee B, Purdy AJ, Halverson GH, Dohlen MB, Cawse–Nicholson K, Wang A, Anderson RG, Aragon B, Arain MA, et al. 2020. ECOSTRESS: NASA's next generation mission to measure evapotranspiration from the International Space Station. *Water Resour Res*. [accessed 2022 Oct 14];56(4):e2019WR02605. <https://doi.org/10.1029/2019WR026058>
- Franke J, Roberts DA, Halligan K, Menz G. 2009. Hierarchical Multiple Endmember Spectral Mixture Analysis (MESMA) of hyperspectral imagery for urban environments. *Remote Sens Environ*. [accessed 2022 Oct 14];113(8):1712–1723. <https://doi.org/10.1016/j.rse.2009.03.018>
- Franklin SE, Wulder MA, Gerylo GR. 2001. Texture analysis of IKONOS panchromatic data for Douglas-fir forest age class separability in British Columbia. *Intl J Remote Sens*. [accessed 2022 Oct 14];22(13):2627–2632. <https://doi.org/10.1080/01431160120769>
- Frazier AE. 2015. Landscape heterogeneity and scale considerations for super-resolution mapping. *Intl J Remote Sens*. [accessed 2022 Oct 14];36(9):2395–2408. <https://doi.org/10.1080/2150704X.2015.1040130>

- Frazier AE, Wang L. 2011. Characterizing spatial patterns of invasive species using sub-pixel classifications. *Remote Sens Environ.* [accessed 2022 Oct 14];115(8):1997–2007. <https://doi.org/10.1016/j.rse.2011.04.002>
- Gamon JA. 2015. Reviews and syntheses: optical sampling of the flux tower footprint. *Biogeosci.* [accessed 2022 Oct 14];12(14):4509–4523. <https://doi.org/10.5194/bg-12-4509-2015>
- [GEO] Group on Earth Observations 2015. The value of open data sharing. GEO Participating Organization CODATA. Geneva. 44 p. [accessed 2022 Oct 14]. Available from: https://www.earthobservations.org/documents/dsp/20151130_the_value_of_open_data_sharing.pdf
- Giardino C, Brando VE, Dekker AG, Strömbeck N, Candiani G. 2007. Assessment of water quality in Lake Garda (Italy) using Hyperion. *Remote Sens Environ.* [accessed 2022 Oct 14];109(2):183–195. <https://doi.org/10.1016/j.rse.2006.12.017>
- Giardino C, Brando VE, Gege P, Pinnel N, Hochberg E, Knaeps E, Reusen I, Doerffer R, Bresciani M, Braga F, et al. 2019. Imaging spectrometry of inland and coastal waters: state of the art, achievements and perspectives. *Surv Geophys.* [accessed 2022 Oct 14];40(3):401–429. <https://doi.org/10.1007/s10712-018-9476-0>
- Gilerson A, Herrera–Estrella E, Foster R, Agagiate J, Hu C, Ibrahim A, Franz B. 2022. Determining the primary sources of uncertainty in retrieval of marine remote sensing reflectance from satellite ocean color sensors. *Front Remote Sens.* [accessed 2022 Oct 14];3:857530. <https://doi.org/10.3389/frsen.2022.857530>
- Gilerson A, Zhou J, Hlaing S, Ioannou I, Schalles J, Gross B, Moshary F, Ahmed S. 2007. Fluorescence component in the reflectance spectra from coastal waters. Dependence on water composition. *Opt Express.* [accessed 2022 Oct 14];15(24):15702–15721. <https://doi.org/10.1364/OE.15.015702>
- Gitelson AA, Viña A, Verma SB, Rundquist DC, Arkebauer TJ, Keydan G, Leavitt B, Ciganda V, Burba GG, Suyker AE. 2006. Relationship between gross primary production and chlorophyll content in crops: implications for the synoptic monitoring of vegetation productivity. *J Geophys Res: Atmos.* [accessed 2022 Oct 14];111(D8). <https://doi.org/10.1029/2005JD006017>
- Greenberg JA, Hestir EL, Riano D, Scheer GJ, Ustin SL. 2012. Using LiDAR Data Analysis to Estimate changes in insolation under large-scale riparian deforestation. *J Am Water Resour Assoc.* [accessed 2022 Oct 14];48(5):939–948. <https://doi.org/10.1111/j.1752-1688.2012.00664.x>
- Groom S, Sathyendranath S, Ban Y, Bernard S, Brewin R, Brotas V, Brockmann C, Chauhan P, Choi J, Chuprin A, et al. 2019. Satellite ocean colour: current status and future perspective. *Front Mar Sci.* [accessed 2022 Oct 14];6:485. <https://doi.org/10.3389/fmars.2019.00485>
- Guild LS, Kudela RM, Hooker SB, Palacios SL, Houskeeper HF. 2020. Airborne radiometry for calibration, validation, and research in oceanic, coastal, and inland waters. *Front Environ Sci.* [accessed 2022 Oct 14];8:209. <https://doi.org/10.3389/fenvs.2020.585529>
- Gupana RS, Odermatt D, Cesana I, Giardino C, Nedbal L, Damm A. 2021. Remote sensing of sun-induced chlorophyll a fluorescence in inland and coastal waters: current state and future prospects. *Remote Sens Environ.* [accessed 2022 Oct 14];262:112482. <https://doi.org/10.1016/j.rse.2021.112482>
- Gustine RN, Lee CM, Acuna SC, Cawse–Nicholson K, Hulley G, Hestir EL. 2021. Using ECOSTRESS to observe and model diurnal variability in water temperature conditions in the San Francisco estuary. *IEEE Trans Geosci Remote Sens.* [accessed 2022 Oct 14];60:1–10. <https://doi.org/10.1109/TGRS.2021.3133411>
- Halverson GH, Lee CM, Hestir EL, Hulley G, Cawse–Nicholson K, Hook SJ, Bergamaschi BA, Acuna SC, Truffilario N, Radocinski R, et al. 2021. Decline in thermal habitat conditions for the endangered Delta Smelt as seen from Landsat satellites (1985–2019). *Environ Sci Technol.* [accessed 2022 Oct 14];56(1):185–193. <https://doi.org/10.1021/acs.est.1c02837>
- Hemes KS, Chamberlain SD, Eichelmann E, Anthony T, Valach A, Kasak K, Szutu D, Verfaillie J, Silver WL, Baldocchi DD. 2019. Assessing the carbon and climate benefit of restoring degraded agricultural peat soils to managed wetlands. *Agric For Meteorol.* [accessed 2022 Oct 14]; 268:202–214. <https://doi.org/10.1016/j.agrformet.2019.01.017>

- Henderson FM, Lewis AJ. 2008. Radar detection of wetland ecosystems: a review. *Intl J Remote Sen.* [accessed 2022 Oct 14];29(20):5809–5835. <https://doi.org/10.1080/01431160801958405>
- Hestir EL, Brando VE, Bresciani M, Giardino C, Matta E, Villa P, Dekker AG. 2015. Measuring freshwater aquatic ecosystems: the need for a hyperspectral global mapping satellite mission. *Remote Sens Environ.* [accessed 2022 Oct 14]; 167:181–195. <https://doi.org/10.1016/j.rse.2015.05.023>
- Hestir EL, Greenberg JA, Ustin SL. 2012. Classification trees for aquatic vegetation community prediction from imaging spectroscopy. *IEEE J Sel Top Appl Earth Obs Remote Sens.* [accessed 2022 Oct 14]; 5(5):1572–1584. <https://doi.org/10.1109/JSTARS.2012.2200878>
- Hestir EL, Khanna S, Andrew ME, Santos MJ, Viers JH, Greenberg JA, Rajapakse SS, Ustin SL. 2008. Identification of invasive vegetation using hyperspectral remote sensing in the California Delta ecosystem. *Remote Sens Environ.* [accessed 2022 Oct 14];112(11):4034–4047. <https://doi.org/10.1016/j.rse.2008.01.022>
- Hestir EL, Schoellhamer DH, Greenberg J, Morgan-King T, Ustin SL. 2016. The effect of submerged aquatic vegetation expansion on a declining turbidity trend in the Sacramento–San Joaquin River Delta. *Estuaries Coasts.* [accessed 2022 Oct 14];39:1100–1112. <https://doi.org/10.1007/s12237-015-0055-z>
- Hickson D, Keeler-Wolf T. 2007. Vegetation and land-use classification and map of the Sacramento–San Joaquin River Delta. Report to the Bay Delta Region of the California Dept. of Fish and Game. Sacramento (CA): CDFG. [accessed 2022 Oct 14] 283 p. Available from: <https://nrm.dfg.ca.gov/FileHandler.ashx?DocumentID=18211>
- Homolová L, Malenovský Z, Clevers JGPW, García-Santos G, Schaepman ME. 2013. Review of optical-based remote sensing for plant trait mapping. *Ecol Complex.* [accessed 2022 Oct 14]; 15:1–16. <https://doi.org/10.1016/j.ecocom.2013.06.003>
- Hoogenboom HJ, Dekker AG, Althuis IJA. 1998. Simulation of AVIRIS sensitivity for detecting chlorophyll over coastal and inland waters. *Remote Sens Environ.* [accessed 2022 Oct 14];65(3):333–340. [https://doi.org/10.1016/S0034-4257\(98\)00042-X](https://doi.org/10.1016/S0034-4257(98)00042-X)
- Hossain MD, Chen D. 2019. Segmentation for Object-Based Image Analysis (OBIA): a review of algorithms and challenges from remote sensing perspective. *ISPRS J Photogram Remote Sens.* [accessed 2022 Oct 14];150:115–134. <https://doi.org/10.1016/j.isprsjprs.2019.02.009>
- Huang S, Tang L, Hupy JP, Wang Y, Shao G. 2021. A commentary review on the use of normalized difference vegetation index (NDVI) in the era of popular remote sensing. *J For Res.* [accessed 2022 Oct 14];32(1):1–6. <https://doi.org/10.1007/s11676-020-01155-1>
- Huete A, Didan K, Miura T, Rodriguez EP, Gao X, Ferreira LG. 2002. Overview of the radiometric and biophysical performance of the MODIS vegetation indices. *Remote Sens Environ.* [accessed 2022 Oct 14];83(1–2):195–213. [https://doi.org/10.1016/S0034-4257\(02\)00096-2](https://doi.org/10.1016/S0034-4257(02)00096-2)
- Jensen D, Simard M, Cavanaugh K, Sheng Y, Fichot CG, Pavelsky T, Twilley R. 2019. Improving the transferability of suspended solid estimation in wetland and deltaic waters with an empirical hyperspectral approach. *Remote Sensing.* [accessed 2022 Oct 14];11(13). <https://doi.org/10.3390/rs11131629>
- Jing R, Gong Z, Zhao W, Pu R, Deng L. 2017. Above-bottom biomass retrieval of aquatic plants with regression models and SfM data acquired by a UAV platform – a case study in Wild Duck Lake Wetland, Beijing, China. *ISPRS J Photogram Remote Sens.* [accessed 2022 Oct 14];134:122–134. <https://doi.org/10.1016/j.isprsjprs.2017.11.002>
- Kalacska M, Chmura GL, Lucanus O, Bérubé D, Arroyo-Mora JP. 2017. Structure from motion will revolutionize analyses of tidal wetland landscapes. *Remote Sens Environ.* [accessed 2022 Oct 14];199:14–24. <https://doi.org/10.1016/j.rse.2017.06.023>
- Kearney MS, Stutzer D, Turpie K, Stevenson JC. 2009. The effects of tidal inundation on the reflectance characteristics of coastal marsh vegetation. *J Coastal Res.* [accessed 2022 Oct 14];256:1177–1186. <https://doi.org/10.2112/08-1080.1>

- Kelly M, Tuxen KA, Stralberg D. 2011. Mapping changes to vegetation pattern in a restoring wetland: finding pattern metrics that are consistent across spatial scale and time. *Ecol Indicators*. [accessed 2022 Oct 14];11(2):263–273. <https://doi.org/10.1016/j.ecolind.2010.05.003>
- Kennedy RE, Townsend PA, Gross JE, Cohen WB, Bolstad P, Wang YQ, Adams P. 2009. Remote sensing change detection tools for natural resource managers: understanding concepts and tradeoffs in the design of landscape monitoring projects. *Remote Sens Environ*. [accessed 2022 Oct 14];113(7):1382–1396. <https://doi.org/10.1016/j.rse.2008.07.018>
- Khanna S. 2010. Development and use of remote sensing tools to study the impact of water hyacinth (*Eichhornia crassipes*) invasion in an estuarine ecosystem. [dissertation]. [Davis (CA)]: University of California. 24 p. [accessed 2022 Oct 14]. Available from: <https://www.proquest.com/dissertations-theses/development-use-remote-sensing-tools-study-impact/docview/808524493/se-2>
- Khanna S, Santos MJ, Boyer JD, Shapiro KD, Bellvert J, Ustin SL. 2018. Water primrose invasion changes successional pathways in an estuarine ecosystem. *Ecosphere*. [accessed 2022 Oct 14]; 9(9):e02418. <https://doi.org/10.1002/ecs2.2418>
- Khanna S, Santos MJ, Hestir EL, Ustin SL. 2012. Plant community dynamics relative to the changing distribution of a highly invasive species, *Eichhornia crassipes*: a remote sensing perspective. *Biol Invasions*. [accessed 2022 Oct 14];14(3):717–733. <https://doi.org/10.1007/s10530-011-0112-x>
- Khanna S, Santos MJ, Ustin SL, Haverkamp PJ. 2011. An integrated approach to a biophysically based classification of floating aquatic macrophytes. *Intl J Remote Sens*. [accessed 2022 Oct 14];32(4):1067–1094. <https://doi.org/10.1080/01431160903505328>
- Khorram S, Koch FH, van der Wiele CF, Nelson SAC. 2012. Data acquisition. In: Khorram S, Nelson SAC, Koch FH, van der Wiele CF (editors). *Remote sensing*. Boston (MA): Springer US. [accessed 2022 Oct 14]; p 17–37. https://doi.org/10.1007/978-1-4614-3103-9_2
- Kimmerer W, Wilkerson F, Downing B, Dugdale R, Gross E, Kayfetz K, Khanna S, Parker A, Thompson J. 2019. Effects of drought and the emergency drought barrier on the ecosystem of the California Delta. *San Franc estuary Watershed Sci*. [accessed 2022 Oct 14];17(3). <https://doi.org/10.15447/sfews.2019v17iss3art2>
- Knight JF, Lunetta RS. 2003. An experimental assessment of minimum mapping unit size. *IEEE Trans Geosci Remote Sens*. [accessed 2022 Oct 14];41(9):2132–2134. <https://doi.org/10.1109/TGRS.2003.816587>
- Knox SH, Dronova I, Sturtevant C, Oikawa PY, Matthes JH, Verfaillie J, Baldocchi D. 2017. Using digital camera and Landsat imagery with eddy covariance data to model gross primary production in restored wetlands. *Agric For Meteorol*. [accessed 2022 Oct 14];237–238:233–245. <https://doi.org/10.1016/j.agrformet.2017.02.020>
- Knox SH, Matthes JH, Sturtevant C, Oikawa PY, Verfaillie J, Baldocchi D. 2016. Biophysical controls on interannual variability in ecosystem-scale CO₂ and CH₄ exchange in a California rice paddy: Interannual variability rice CH₄ fluxes. *J Geophys Res: Biogeosci*. [accessed 2022 Oct 14];121(3):978–1001. <https://doi.org/10.1002/2015JG003247>
- Knox SH, Sturtevant C, Matthes JH, Koteen L, Verfaillie J, Baldocchi D. 2015. Agricultural peatland restoration: effects of land-use change on greenhouse gas (CO₂ and CH₄) fluxes in the Sacramento–San Joaquin Delta. *Glob Change Biol*. [accessed 2022 Oct 14];21(2):750–765. <https://doi.org/10.1111/gcb.12745>
- Kraus TEC, Bergamaschi BA, Downing BD. 2017. An introduction to high-frequency nutrient and biogeochemical monitoring for the Sacramento–San Joaquin Delta, northern California. United States Geological Survey Technical Report 2017-5071. Reston (VA): USGS. [accessed 2022 Oct 14] 41 p. <https://doi.org/10.3133/sir20175071>
- Kristensen T, Næsset E, Ohlson M, Bolstad PV, Kolka R. 2015. Mapping above- and below-ground carbon pools in boreal forests: the case for airborne lidar. *PLoS ONE*. [accessed 2022 Oct 14];10(10):e0138450. <https://doi.org/10.1371/journal.pone.0138450>

- Kudela RM, Palacios SL, Austerberry DC, Accorsi EK, Guild LS, Torres-Perez J. 2015. Application of hyperspectral remote sensing to cyanobacterial blooms in inland waters. *Remote Sens Environ.* [accessed 2022 Oct 14];167:196–205. <https://doi.org/10.1016/j.rse.2015.01.025>
- Lee CM, Hestir EL, Tuffillaro N, Palmieri B, Acuña S, Osti A, Bergamaschi BA, Sommer T. 2021. Monitoring turbidity in San Francisco estuary and Sacramento–San Joaquin Delta using satellite Remote Sens. *J Am Water Resour Assoc.* [accessed 2022 Oct 14];57(5):737–751. <https://doi.org/10.1111/1752-1688.12917>
- Lekki J, Deutsch E, Sayers M, Bosse K, Anderson R, Tokars R, Sawtell R. 2019. Determining remote sensing spatial resolution requirements for the monitoring of harmful algal blooms in the Great Lakes. *J Great Lakes Res.* [accessed 2022 Oct 14];45(3):434–443. <https://doi.org/10.1016/j.jglr.2019.03.014>
- Li H, Zhang C, Zhang S, Atkinson PM. 2019. Full year crop monitoring and separability assessment with fully-polarimetric L-band UAVSAR: a case study in the Sacramento Valley, California. *Intl J Appl Earth Obs Geoinfo.* [accessed 2022 Oct 14];74:45–56. <https://doi.org/10.1016/j.jag.2018.08.024>
- Li L, Qiang Y, Zheng Z, Zhang J. 2019. Research on the relationship between the spatial resolution and the map scale in the satellite remote sensing cartographies. *Proceedings of the 2019 international conference on Modeling, Analysis, Simulation Technologies and Applications (MASTA 2019)*. 2019 May 26–27 Hangzhou. Paris (FR): Atlantis Press. [accessed 2022 Oct 14]. p 194–199. <https://doi.org/10.2991/masta-19.2019.33>
- Li L, Ustin SL, Lay M. 2005. Application of multiple endmember spectral mixture analysis (MESMA) to AVIRIS imagery for coastal salt marsh mapping: a case study in China Camp, CA, USA. *Intl J Remote Sens.* [accessed 2022 Oct 14];26(23):5193–5207. <https://doi.org/10.1080/01431160500218911>
- Liao T-H, Simard M, Denbina M, Lamb MP. 2020. Monitoring water level change and seasonal vegetation change in the coastal wetlands of Louisiana using L-Band time-series. *Remote Sens.* [accessed 2022 Oct 14];12(15). <https://doi.org/10.3390/rs12152351>
- Lopatin J, Kattenborn T, Galleguillos M, Perez-Quezada JF, Schmidtlein S. 2019. Using aboveground vegetation attributes as proxies for mapping peatland belowground carbon stocks. *Remote Sens Environ.* [accessed 2022 Oct 14];231(15):111217. <https://doi.org/10.1016/j.rse.2019.111217>
- Madritch M, Cavender-Bares J, Hobbie SE, Townsend PA. 2020. Linking foliar traits to belowground processes. In: Cavender-Bares J, Gamon JA, Townsend PA (editors). *Remote sensing of plant biodiversity*. Cham: Springer International Publishing. [accessed 2022 Oct 14]; p 173–197. https://doi.org/10.1007/978-3-030-33157-3_8
- Madritch MD, Kingdon CC, Singh A, Mock KE, Lindroth RL, Townsend PA. 2014. Imaging spectroscopy links aspen genotype with below-ground processes at landscape scales. *Philos Trans Royal Soc B: Biol Sci.* [accessed 2022 Oct 14];369(1643):20130194. <https://doi.org/10.1098/rstb.2013.0194>
- Matthes JH, Knox SH, Sturtevant C, Sonnentag O, Verfaillie J, Baldocchi D. 2015. Predicting landscape-scale CO₂ flux at a pasture and rice paddy with long-term hyperspectral canopy reflectance measurements. *Biogeosciences.* [accessed 2022 Oct 14];12:4577–4594. <https://doi.org/10.5194/bg-12-4577-2015>
- Matthes JH, Sturtevant C, Verfaillie J, Knox S, Baldocchi D. 2014. Parsing the variability in CH₄ flux at a spatially heterogeneous wetland: integrating multiple eddy covariance towers with high-resolution flux footprint analysis. *J Geophys Res–Biogeosci.* [accessed 2022 Oct 14];119(7):1322–1339. <https://doi.org/10.1002/2014JG002642>
- McCarthy MJ, Colna KE, El-Mezayen MM, Laureano-Rosario AE, Méndez-Lázaro P, Otis DB, Toro-Farmer G, Vega-Rodríguez M, Muller-Karger FE. 2017. Satellite remote sensing for coastal management: a review of successful applications. *Environ Manag.* [accessed 2022 Oct 14];60(2):323–339. <https://doi.org/10.1007/s00267-017-0880-x>

- McNicol G, Sturtevant CS, Knox SH, Dronova I, Baldocchi DD, Silver WL. 2017. Effects of seasonality, transport pathway, and spatial structure on greenhouse gas fluxes in a restored wetland. *Glob Change Biol.* [accessed 2022 Oct 14];23(7):2768–2782. <https://doi.org/10.1111/gcb.13580>
- Medeiros S, Hagen S, Weishampel J, Angelo J. 2015. Adjusting Lidar-derived digital terrain models in coastal marshes based on estimated Aboveground biomass density. *Remote Sens.* [accessed 2022 Oct 14];7(4):3507–3525. <https://doi.org/10.3390/rs70403507>
- Méléder V, Savelli R, Barnett A, Polsenaeere P, Gernez P, Cugier P, Lerouxel A, le Bris A, Dupuy C, le Fouest V, et al. 2020. Mapping the intertidal microphytobenthos gross primary production part I: coupling multispectral remote sensing and physical modeling. *Front Mar Sci.* [accessed 2022 Oct 14];7:520. <https://doi.org/10.3389/fmars.2020.00520>
- Mercury M, Green R, Hook S, Oaida B, Wu W, Gunderson A, Chodas M. 2012. Global cloud cover for assessment of optical satellite observation opportunities: a HypSPIRI case study. *Remote Sens Environ.* [accessed 2022 Oct 14];126:62–71. <https://doi.org/10.1016/j.rse.2012.08.007>
- Moffett KB, Gorelick SM. 2013. Distinguishing wetland vegetation and channel features with object-based image segmentation. *Intl J Remote Sens.* [accessed 2022 Oct 14];34(4):1332–1354. <https://doi.org/10.1080/01431161.2012.718463>
- Mohammed GH, Colombo R, Middleton EM, Rascher U, van der Tol C, Nedbal L, Goulas Y, Pérez-Priego O, Damm A, Meroni M, et al. 2019. Remote sensing of solar-induced chlorophyll fluorescence (SIF) in vegetation: 50 years of progress. *Remote Sens Environ.* [accessed 2022 Oct 14];231:111177. <https://doi.org/10.1016/j.rse.2019.04.030>
- Morton DC, Nagol J, Carabajal CC, Rosette J, Palace M, Cook BD, Vermote EF, Harding DJ, North PRJ. 2014. Amazon forests maintain consistent canopy structure and greenness during the dry season. *Nature.* [accessed 2022 Oct 14];506(7487):221–224. <https://doi.org/10.1038/nature13006>
- Moses WJ, Sterckx S, Montes M J, De Keukelaere L, Knaeps E. 2017. Atmospheric correction for inland waters. Chapter 3. In: Mishra D, Ogashawara I, Gitelson A, editors. *Bio-optical modeling and remote sensing of inland waters.* Elsevier. [accessed 2022 Oct 14]; p. 69–100. <https://doi.org/10.1016/B978-0-12-804644-9.00003-3>
- Mouw CB, Greb S, Aurin D, DiGiacomo PM, Lee Z, Twardowski M, Binding C, Hu C, Ma R, Moore T, et al. 2015. Aquatic color radiometry remote sensing of coastal and inland waters: challenges and recommendations for future satellite missions. *Remote Sens Environ.* [accessed 2022 Oct 14];160:15–30. <https://doi.org/10.1016/j.rse.2015.02.001>
- Muller-Karger FE, Hestir E, Ade C, Turpie K, Roberts DA, Siegel D, Miller RJ, Humm D, Izenberg N, Keller M, et al. 2018. Satellite sensor requirements for monitoring essential biodiversity variables of coastal ecosystems. *Ecol Appl.* [accessed 2022 Oct 14];28(3):749–760. <https://doi.org/10.1002/eap.1682>
- Næsset E, Gobakken T. 2008. Estimation of above- and below-ground biomass across regions of the boreal forest zone using airborne laser. *Remote Sens Environ.* [accessed 2022 Oct 14];112(6):3079–3090. <https://doi.org/10.1016/j.rse.2008.03.004>
- O’Connell J, Byrd K, Kelly M. 2015. A hybrid model for mapping relative differences in belowground biomass and root: shoot ratios using spectral reflectance, foliar N and plant biophysical data within coastal marsh. *Remote Sens.* [accessed 2022 Oct 14];7(12):16480–16503. <https://doi.org/10.3390/rs71215837>
- Oikawa PY, Jenerette GD, Knox SH, Sturtevant C, Verfaillie J, Dronova I, Poindexter CM, Eichelmann E, Baldocchi DD. 2017. Evaluation of a hierarchy of models reveals importance of substrate limitation for predicting carbon dioxide and methane exchange in restored wetlands. *J Geophys Res: Biogeosci.* [accessed 2022 Oct 14];122(1):145–167. <https://doi.org/10.1002/2016JG003438>
- Ollinger SV. 2011. Sources of variability in canopy reflectance and the convergent properties of plants. *New Phytol.* [accessed 2022 Oct 14];189(2):375–394. <https://doi.org/10.1111/j.1469-8137.2010.03536.x>

- Ozesmi SL, Bauer ME. 2002. Satellite remote sensing of wetlands. *Wetl Ecol Manag.* [accessed 2022 Oct 14];10(5):381–402.
<https://doi.org/10.1023/A:1020908432489>
- Pahlevan N, Chittimalli SK, Balasubramanian SV, Vellucci V. 2019. Sentinel-2/Landsat-8 product consistency and implications for monitoring aquatic systems. *Remote Sens Environ.* [accessed 2022 Oct 14];220:19–29.
<https://doi.org/10.1016/j.rse.2018.10.027>
- Palacios SL, Kudela RM, Guild LS, Negrey KH, Torres–Perez J, Broughton J. 2015. Remote sensing of phytoplankton functional types in the coastal ocean from the HyspIRI preparatory flight campaign. *Remote Sens Environ.* [accessed 2022 Oct 14];167:269–280.
<https://doi.org/10.1016/j.rse.2015.05.014>
- Paterson DM, Wiltshire KH, Miles A, Blackburn J, Davidson I, Yates MG, McGrorty S, Eastwood JA. 1998. Microbiological mediation of spectral reflectance from intertidal cohesive sediments. *Limnol Oceanogr.* [accessed 2022 Oct 14];43(6):1207–1221.
<https://doi.org/10.4319/lo.1998.43.6.1207>
- Pellerin B. 2015. Applications of optical sensors for high-frequency water-quality monitoring and research. United States Geological Survey. [accessed 2022 Oct 14];1 p. Available from:
<https://pubs.er.usgs.gov/publication/70156710>
- Pettorelli N, Wegmann M, Skidmore A, Mùcher S, Dawson TP, Fernandez M, Lucas R, Schaepman ME, Wang T, O'Connor B, et al. 2016. Framing the concept of satellite remote sensing essential biodiversity variables: challenges and future directions. *Remote Sens Ecol Conserv.* [accessed 2022 Oct 14];2(3):122–131.
<https://doi.org/10.1002/rse2.15>
- Price JC. 1997. Spectral band selection for visible–near infrared remote sensing: spectral–spatial resolution tradeoffs. *IEEE Trans Geosci Remote Sens.* [accessed 2022 Oct 14];35(5):1277–1285.
<https://doi.org/10.1109/36.628794>
- Quinn NWT, Epshtein O. 2014. Seasonally-managed wetland footprint delineation using Landsat ETM+ satellite imagery. *Environ Model Softw.* [accessed 2022 Oct 14];54:9–23.
<https://doi.org/10.1016/j.envsoft.2013.12.012>
- Reinke K, Jones S. 2006. Integrating vegetation field surveys with remotely sensed data. *Ecol Manag Restor.* [accessed 2022 Oct 14];7(s1):S18–S23.
<https://doi.org/10.1111/j.1442-8903.2006.00287.x>
- Reisi–Gahrouei O, Homayouni S, McNairn H, Hosseini M, Safari A. 2019. Crop biomass estimation using multi regression analysis and neural networks from multitemporal L-band polarimetric synthetic aperture radar data. *Intl J Remote Sens.* [accessed 2022 Oct 14];40(17):6822–6840. <https://doi.org/10.1080/01431161.2019.1594436>
- Robinson AH, Safran, S, Beagle J, Grossinger, R, Grenier, J, Askevold, R. 2014. A Delta transformed: ecological functions, spatial metrics, and landscape change in the Sacramento–San Joaquin Delta. SFEI Contribution No. 729. Richmond (CA): San Francisco estuary Institute–Aquatic Science Center (SFEI–ASC). [accessed 2022 Oct 14];155 p. Available from:
<https://www.sfei.org/documents/delta-transformed-ecological-functions-spatial-metrics-and-landscape-change-sacramento-san>
- Rogers JN, Parrish CE, Ward LG, Burdick DM. 2015. Evaluation of field-measured vertical obscuration and full waveform lidar to assess salt marsh vegetation biophysical parameters. *Remote Sens Environ.* [accessed 2022 Oct 14];156:264–275.
<https://doi.org/10.1016/j.rse.2014.09.035>
- Rogers JN, Parrish CE, Ward LG, Burdick DM. 2018. Improving salt marsh digital elevation model accuracy with full-waveform lidar and nonparametric predictive modeling. *Estuar Coast Shelf Sci.* [accessed 2022 Oct 14];202:193–211.
<https://doi.org/10.1016/j.ecss.2017.11.034>
- Rosso PH, Ustin SL, Hastings A. 2005. Mapping marshland vegetation of San Francisco Bay, California, using hyperspectral data. *Intl J Remote Sens.* [accessed 2022 Oct 14];26(23):5169–5191.
<https://doi.org/10.1080/01431160500218770>
- Rosso PH, Ustin SL, Hastings A. 2006. Use of lidar to study changes associated with *Spartina* invasion in San Francisco Bay marshes. *Remote Sens Environ.* [accessed 2022 Oct 14];100(3):295–306.
<https://doi.org/10.1016/j.rse.2005.10.012>

- Rouse JW, Haas RH, Scheel JA, Deering DW. 1974. Monitoring vegetation systems in the Great Plains with ERTS. Proceedings, Third Earth Resource Technology Satellite-1 Symposium (ERTS) Symposium. Volume 1: Technical Presentations, section A. [accessed 2022 Oct 14];1:48–62. Available from: <https://ntrs.nasa.gov/citations/19740022614>
- Ryan PJ, Davis OC, Tufillaro BN, Kudela MR, Gao B–C. 2014. Application of the hyperspectral imager for the coastal ocean to phytoplankton ecology studies in Monterey Bay, CA, USA. *Remote Sens.* [accessed 2022 Oct 14];6(2). <https://doi.org/10.3390/rs6021007>
- Ryu Y, Baldocchi DD, Kobayashi H, van Ingen C, Li J, Black TA, Beringer J, van Gorsel E, Knohl A, Law BE, et al. 2011. Integration of MODIS land and atmosphere products with a coupled-process model to estimate gross primary productivity and evapotranspiration from 1 km to global scales. *Global Biogeochem Cycles.* [accessed 2022 Oct 14];25(4):GB4017. <https://doi.org/10.1029/2011GB004053>
- Salama Mhd S, Stein A. 2009. Error decomposition and estimation of inherent optical properties. *Appl Opt.* [accessed 2022 Oct 14];48(26):4947–4962. <https://doi.org/10.1364/AO.48.004947>
- Samanta A, Ganguly S, Hashimoto H, Devadiga S, Vermote E, Knyazikhin Y, Nemani RR, Myneni RB. 2010. Amazon forests did not green-up during the 2005 drought. *Geophys Res Lett.* [accessed 2022 Oct 14];37(5). <https://doi.org/10.1029/2009GL042154>
- Santos MJ, Hestir EL, Khanna S, Ustin SL. 2012. Image spectroscopy and stable isotopes elucidate functional dissimilarity between native and nonnative plant species in the aquatic environment. *New Phytol.* [accessed 2022 Oct 14];193(3):683–695. <https://doi.org/10.1111/j.1469-8137.2011.03955.x>
- Santos MJ, Khanna S, Hestir EL, Andrew ME, Rajapakse SS, Greenberg JA, Anderson LWJ, Ustin SL. 2009. Use of hyperspectral remote sensing to evaluate efficacy of aquatic plant management. *Invasive Plant Sci Manag.* [accessed 2022 Oct 14];2(3):216–229. <https://doi.org/10.1614/IPSM-08-115.1>
- Santos MJ, Khanna S, Hestir EL, Greenberg JA, Ustin SL. 2016. Measuring landscape-scale spread and persistence of an invaded submerged plant community from airborne remote sensing. *Ecol Appl.* [accessed 2022 Oct 14];26(6):1733–1744. <https://doi.org/10.1890/15-0615>
- Saraceno JF, Pellerin BA, Downing BD, Boss E, Bachand PAM, Bergamaschi BA. 2009. High-frequency *in situ* optical measurements during a storm event: assessing relationships between dissolved organic matter, sediment concentrations, and hydrologic processes. *J Geophys Res: Biogeosci.* [accessed 2022 Oct 14];114(G4). <https://doi.org/10.1029/2009JG000989>
- Saura S. 2002. Effects of minimum mapping unit on land cover data spatial configuration and composition. *Intl J Remote Sens.* [accessed 2022 Oct 14];23(22):4853–4880. <https://doi.org/10.1080/01431160110114493>
- Schile LM, Callaway JC, Morris JT, Stralberg D, Parker VT, Kelly M. 2014. Modeling tidal marsh distribution with sea-level rise: evaluating the role of vegetation, sediment, and upland habitat in marsh resiliency. *PLoS ONE.* [accessed 2022 Oct 14];9(2):e88760. <https://doi.org/10.1371/journal.pone.0088760>
- Schweiger AK, Cavender–Bares J, Townsend PA, Hobbie SE, Madritch MD, Wang R, Tilman D, Gamon JA. 2018. Plant spectral diversity integrates functional and phylogenetic components of biodiversity and predicts ecosystem function. *Nature Ecol Evol.* [accessed 2022 Oct 14];2(6):976–982. <https://doi.org/10.1038/s41559-018-0551-1>
- Seavy NE, Viers JH, Wood JK. 2009. Riparian bird response to vegetation structure: a multiscale analysis using LiDAR measurements of canopy height. *Ecol Appl.* [accessed 2022 Oct 14];19(7):1848–1857. <https://doi.org/10.1890/08-1124.1>
- Sheffield J, Wood EF, Pan M, Beck H, Coccia G, Serrat–Capdevila A, Verbist K. 2018. Satellite remote sensing for water resources management: potential for supporting sustainable development in data-poor regions. *Water Resour Res.* [accessed 2022 Oct 14];54(12):9724–9758. <https://doi.org/10.1029/2017WR022437>

- Simic A, Chen JM, Liu J, Csillag F. 2004. Spatial scaling of net primary productivity using subpixel information. *Remote Sens Environ.* [accessed 2022 Oct 14];93(1):246–258. <https://doi.org/10.1016/j.rse.2004.07.008>
- Stavros EN, Chapman B, Simard M, Osmanoglu B, Jones CE, Hakimdavar R, Jones JW, Bawden G. 2019. 2018 NISAR Applications Workshop: Wetlands. Pasadena (CA): Jet Propulsion Laboratory, CIT/NASA. JPL Publication 19-3. [accessed 2022 Oct 14]. 43 p. Available from: https://nisar.jpl.nasa.gov/system/events/reports/28_2018_NISAR_Wetlands_20190628.pdf
- Stralberg D, Brennan M, Callaway JC, Wood JK, Schile LM, Jongsomjit D, Kelly M, Parker VT, Crooks S. 2011. Evaluating tidal marsh sustainability in the face of sea-level rise: a hybrid modeling approach applied to San Francisco Bay. *PLoS ONE.* [accessed 2022 Oct 14];6(11):e27388. <https://doi.org/10.1371/journal.pone.0027388>
- Stralberg D, Herzog MP, Nur N, Tuxen KA, Kelly M. 2010. Predicting avian abundance within and across tidal marshes using fine-scale vegetation and geomorphic metrics. *Wetlands.* [accessed 2022 Oct 14];30(3):475–487. <https://doi.org/10.1007/s13157-010-0052-8>
- Ta J, Anderson LWJ, Christman M, Khanna S, Kratville D, Madsen J, Moran P, Viers JH. 2017. Invasive aquatic vegetation management in the Sacramento–San Joaquin River Delta: status and recommendations. *San Franc estuary Watershed Sci.* [accessed 2022 Oct 14];15(4). <https://doi.org/10.15447/sfews.2017v15iss4art5>
- Taddeo S, Dronova I. 2019. Geospatial tools for the large-scale monitoring of wetlands in the San Francisco estuary: opportunities and challenges. *San Franc estuary Watershed Sci.* [accessed 2022 Oct 14];17(2). <https://doi.org/10.15447/sfews.2019v17iss2art2>
- Taddeo S, Dronova I. 2020. Landscape metrics of post-restoration vegetation dynamics in wetland ecosystems. *Landsc Ecol.* [accessed 2022 Oct 14];35(2):275–292. <https://doi.org/10.1007/s10980-019-00946-0>
- Taddeo S, Dronova I, Harris K. 2019. The potential of satellite greenness to predict plant diversity among wetland types, ecoregions, and disturbance levels. *Ecol Appl.* [accessed 2022 Oct 14];29(7). <https://doi.org/10.1002/eap.1961>
- Taddeo S, Dronova I, Harris K. 2021. Greenness, texture, and spatial relationships predict floristic diversity across wetlands of the conterminous United States. *ISPRS J Photogram Remote Sens.* [accessed 2022 Oct 14];175:236–246. <https://doi.org/10.1016/j.isprsjprs.2021.03.012>
- Takekawa JY, Woo I, Thorne KM, Buffington KJ, Nur N, Casazza ML, Ackerman JT. 2012. Bird communities: effects of fragmentation, disturbance, and sea level rise on population viability. In: Palaima A (editor). *Ecology, conservation, and restoration of tidal marshes.* Berkeley (CA): University of California Press. [accessed 2022 Oct 14]; p 253–262. <https://doi.org/10.1525/california/9780520274297.003.0018>
- Tao Z, Wang Y, Ma S, Lv T, Zhou X. 2017. A phytoplankton class-specific marine primary productivity model using MODIS data. *IEEE J Sel Top Appl Earth Obs Remote Sens.* [accessed 2022 Oct 14];10(12):5519–5528. <https://doi.org/10.1109/JSTARS.2017.2747770>
- Tarnavsky E, Garrigues S, Brown ME. 2008. Multiscale geostatistical analysis of AVHRR, SPOT-VGT, and MODIS global NDVI products. *Remote Sens Environ.* [accessed 2022 Oct 14];112(2):535–549. <https://doi.org/10.1016/j.rse.2007.05.008>
- Torbick N, Salas WA, Hagen S, Xiao X. 2011. Monitoring rice agriculture in the Sacramento Valley, USA with multitemporal PALSAR and MODIS imagery. *IEEE J Sel Top App Earth Obs Remote Sens.* [accessed 2022 Oct 14];4(2):451–457. <https://doi.org/10.1109/JSTARS.2010.2091493>
- Turner AJ, Köhler P, Magney TS, Frankenberg C, Fung I, Cohen RC. 2020. A double peak in the seasonality of California’s photosynthesis as observed from space. *Biogeosciences.* [accessed 2022 Oct 14];17(2):405–422. <https://doi.org/10.5194/bg-17-405-2020>
- Turpie KR. 2013. Explaining the spectral red-edge features of inundated marsh vegetation. *J Coastal Res.* [accessed 2022 Oct 14];29(5):1111–1117. <https://doi.org/10.2112/JCOASTRES-D-12-00209.1>
- Turpie K, Victor Klemas, Byrd KB, Maggi Kelly, Young–Heon Jo. 2015. Prospective HypsIRI global observations of tidal wetlands. *Remote Sens Environ.* [accessed 2022 Oct 14];167:206–217. <https://doi.org/10.1016/j.rse.2015.05.008>

- Tuxen K, Kelly M. 2008. Multi-scale functional mapping of tidal marsh vegetation using object-based image analysis. In: Blaschke T, Lang S, Hay GJ, editors. Object-based image analysis: spatial concepts for knowledge-driven remote sensing applications. Berlin Heidelberg: Springer. [accessed 2022 Oct 14]; p 415–442.
https://doi.org/10.1007/978-3-540-77058-9_23
- Tuxen K, Schile L, Stralberg D, Siegel S, Parker T, Vasey M, Callaway J, Kelly M. 2011. Mapping changes in tidal wetland vegetation composition and pattern across a salinity gradient using high spatial resolution imagery. *Wetlands Ecol Manag.* [accessed 2022 Oct 14];19(2):141–157.
<https://doi.org/10.1007/s11273-010-9207-x>
- Tuxen KA, Schile LM, Kelly M, Siegel SW. 2008. Vegetation colonization in a restoring tidal marsh: a remote sensing approach. *Restor Ecol.* [accessed 2022 Oct 14];16(2):313–323.
<https://doi.org/10.1111/j.1526-100X.2007.00313.x>
- [USEPA] United States Environmental Protection Agency. 2016. National Wetland Condition: 2011 Assessment Technical Report. EPA-843-R-15-006. Washington, D.C. [accessed 2022 Oct 14]. 279 p. Available from: https://www.epa.gov/sites/default/files/2016-09/documents/nwca_2011_technical_report_-_final_-_may_2016_ver2.pdf
- Underwood E, Ustin S, DiPietro D. 2003. Mapping nonnative plants using hyperspectral imagery. *Remote Sens Environ.* [accessed 2022 Oct 14];86(2):150–161.
[https://doi.org/10.1016/S0034-4257\(03\)00096-8](https://doi.org/10.1016/S0034-4257(03)00096-8)
- Ustin SL, Gamon JA. 2010. Remote sensing of plant functional types. *New Phytologist.* [accessed 2022 Oct 14];186(4):795–816.
<https://doi.org/10.1111/j.1469-8137.2010.03284.x>
- Ustin SL, Middleton EM. 2021. Current and near-term advances in Earth observation for ecological applications. *Ecol Process.* [accessed 2022 Oct 14];10(1):1.
<https://doi.org/10.1186/s13717-020-00255-4>
- Vanhellemont Q, Ruddick K. 2014. Turbid wakes associated with offshore wind turbines observed with Landsat 8. *Remote Sens Environ.* [accessed 2022 Oct 14];145:105–115.
<https://doi.org/10.1016/j.rse.2014.01.009>
- VegCAMP. 2015. Vegetation map update for Suisun Marsh, Solano County, California. A Report to the California Department of Water Resources. [accessed 2022 Oct 14]. Available from: <http://nrm.dfg.ca.gov/FileHandler.ashx?DocumentID=149178>
- Villa P, Bresciani M, Bolpagni R, Pinardi M, Giardino C. 2015. A rule-based approach for mapping macrophyte communities using multi-temporal aquatic vegetation indices. *Remote Sens Environ.* [accessed 2022 Oct 14];171:218–233.
<https://doi.org/10.1016/j.rse.2015.10.020>
- Villa P, Mousivand A, Bresciani M. 2014. Aquatic vegetation indices assessment through radiative transfer modeling and linear mixture simulation. *Intl J Appl Earth Obs Geoinfo.* [accessed 2022 Oct 14];30:113–127.
<https://doi.org/10.1016/j.jag.2014.01.017>
- Wan R, Wang P, Wang X, Yao X, Dai X. 2019. Mapping aboveground biomass of four typical vegetation types in the Poyang Lake Wetlands based on random forest modelling and Landsat images. *Front Plant Sci.* [accessed 2022 Oct 14];10:1281.
<https://doi.org/10.3389/fpls.2019.01281>
- Wedding LM, Moritsch M, Verutes G, Arkema K, Hartge E, Reiblich J, Douglass J, Taylor S, Strong AL. 2021. Incorporating blue carbon sequestration benefits into sub-national climate policies. *Global Environ Change.* [accessed 2022 Oct 14];69:102206.
<https://doi.org/10.1016/j.gloenvcha.2020.102206>
- Westoby MJ, Brasington J, Glasser NF, Hambrey MJ, Reynolds JM. 2012. ‘Structure-from-Motion’ photogrammetry: a low-cost, effective tool for geoscience applications. *Geomorphology.* [accessed 2022 Oct 14];179:300–314.
<https://doi.org/10.1016/j.geomorph.2012.08.021>
- Wicaksono P, Danoedoro P, Hartono, Nehren U. 2016. Mangrove biomass carbon stock mapping of the Karimunjawa Islands using multispectral remote sensing. *Intl J Remote Sens.* [accessed 2022 Oct 14];37(1):26–52.
<https://doi.org/10.1080/01431161.2015.1117679>
- Wood M, de Jong SM, Straatsma MW. 2018. Locating flood embankments using SAR time series: a proof of concept. *Intl J Appl Earth Obs Geoinfo.* [accessed 2022 Oct 14];70:72–83.
<https://doi.org/10.1016/j.jag.2018.04.003>

- [WRMP] Wetland Regional Monitoring Program 2020. San Francisco estuary Wetlands Regional Monitoring Program Plan. Prepared by the WRMP Steering Committee. San Francisco (CA): San Francisco Estuary Partnership. [accessed 2022 Oct 14]; 78 p. Available from: https://www.sfestuary.org/wp-content/uploads/2020/07/SFE_WRMP-Program-Plan_072820_Web.pdf
- Wu Q. 2018. 2.07 - GIS and remote sensing applications in wetland mapping and monitoring. In: Huang B, editor. *Comprehensive Geographic Information Systems*. Oxford: Elsevier. [accessed 2022 Oct 14]; p 140–157. <https://doi.org/10.1016/B978-0-12-409548-9.10460-9>
- Wu W, Zhou Y, Tian B. 2017. Coastal wetlands facing climate change and anthropogenic activities: a remote sensing analysis and modelling application. *Ocean Coast Manag.* [accessed 2022 Oct 14];138:1–10. <https://doi.org/10.1016/j.ocecoaman.2017.01.005>
- Wulder MA, Masek JG, Cohen WB, Loveland TR, Woodcock CE. 2012. Opening the archive: how free data has enabled the science and monitoring promise of Landsat. *Remote Sens Environ.* [accessed 2022 Oct 14];122:2–10. <https://doi.org/10.1016/j.rse.2012.01.010>
- Xiao J, Chevallier F, Gomez C, Guanter L, Hicke JA, Huete AR, Ichii K, Ni W, Pang Y, Rahman AF, et al. 2019. Remote sensing of the terrestrial carbon cycle: a review of advances over 50 years. *Remote Sens Environ.* [accessed 2022 Oct 14];233:111383. <https://doi.org/10.1016/j.rse.2019.111383>
- Xu S, Chen JM, Fernandes R, Cihlar J. 2004. Effects of subpixel water area fraction on mapping leaf area index and modeling net primary productivity in Canada. *Can J Remote Sens.* [accessed 2022 Oct 14];30(5):797–804. <https://doi.org/10.5589/m04-039>
- Yang R–M, Guo W–W. 2019. Modelling of soil organic carbon and bulk density in invaded coastal wetlands using Sentinel-1 imagery. *Intl J Appl Earth Obs Geoinfo.* [accessed 2022 Oct 14];82:101906. <https://doi.org/10.1016/j.jag.2019.101906>
- Zhang M, Ustin SL, Rejmankova E, Sanderson EW. 1997. Monitoring Pacific coast salt marshes using remote sensing. *Ecol Appl.* [accessed 2022 Oct 14];7(3):1039–1053. [https://doi.org/10.1890/1051-0761\(1997\)007\[1039:MPCSMU\]2.0.CO](https://doi.org/10.1890/1051-0761(1997)007[1039:MPCSMU]2.0.CO)
- Zhang X, Friedl MA, Schaaf CB. 2009. Sensitivity of vegetation phenology detection to the temporal resolution of satellite data. *Intl J Remote Sens.* [accessed 2022 Oct 14];30(8):2061–2074. <https://doi.org/10.1080/01431160802549237>
- Zhang Yongguang, Zhang Q, Liu L, Zhang Yangjian, Wang Shaoqiang, Ju W, Zhou G, Zhou L, Tang J, Zhu X, et al. 2021. ChinaSpec: a network for long-term ground-based measurements of solar-induced fluorescence in China. *J Geophys Res: Biogeosci.* [accessed 2022 Oct 14];126(3):e2020JG006042. <https://doi.org/10.1029/2020JG006042>
- Zhu Z, Wulder MA, Roy DP, Woodcock CE, Hansen MC, Radeloff VC, Healey SP, Schaaf C, Hostert P, Strobl P, et al. 2019. Benefits of the free and open Landsat data policy. *Remote Sens Environ.* [accessed 2022 Oct 14];224:382–385. <https://doi.org/10.1016/j.rse.2019.02.016>
- Zibordi G, Mélin F, Berthon J–F, Holben B, Slutsker I, Giles D, D’Alimonte D, Vandemark D, Feng H, Schuster G, et al. 2009. AERONET-OC: a network for the validation of ocean color primary products. *J Atmos Ocean Technol.* [accessed 2022 Oct 14];26(8):1634–1651. <https://doi.org/10.1175/2009JTECHO654.1>
- Zimmerman RC. 2003. A biooptical model of irradiance distribution and photosynthesis in seagrass canopies. *Limnol Oceanogr.* [accessed 2022 Oct 14];48(1part2):568–585. https://doi.org/10.4319/lo.2003.48.1_part_2.0568
- Zomer RJ, Trabucco A, Ustin SL. 2009. Building spectral libraries for wetlands land cover classification and hyperspectral remote sensing. *J Environ Manag.* [accessed 2022 Oct 14];90(7):2170–2177. <https://doi.org/10.1016/j.jenvman.2007.06.028>